COS Calibration Requirements & Procedures

Date:	May 20, 2002
Document Number:	COS-01-0003
Revision:	Revision B
Contract No.:	NAS5-98043
CDRL No.:	AV-03

Prepared By:	Erik Wilkinson	1-31-01
	Dr. Erik Wilkinson, COS Instrument Scientist	Date
Reviewed By:	Dennis Ebbets	2-15-01
	Dr. Dennis Ebbets, COS Calibration Scientist, BASD	Date
Reviewed By:	Jon A. Morse	2-1-01
	Dr. Jon Morse, COS Project Scientist	Date
Approved By:	James C. Green	2-5-01
	Dr. James C. Green, COS Principal Investigator	Date
Approved By:	John Paul Andrews	2-9-01
	Mr. John Andrews, COS Experiment Manager	Date

Center for Astrophysics & Space Astronomy
University of Colorado
Campus Box 593
Boulder, Colorado 80309

REVISIONS

Letter	ECO No.	Description	Check	Approved	Date
-		Initial Release		EW	1-31-01
A	COS-060	Changes detailed on ECO		EW	4-2-01
B	COS-074	Changes detailed on ECO			

Original Release Name	Date
Drawn: E. Wilkinson	1-29-01
Reviewed:	
Approved:	

THE UNIVERSITY OF COLORADO

At Boulder

The Center for Astrophysics and Space Astronomy

COS Calibration Requirements Document (AV-03)

Size	Code Indent No.	Document No.	Rev
A		COS-01-0003	B
Scale: N/A			

Table of Contents

ACRONYM LIST

ACCUM	Refers to a data set acquired as a histogram
ADQ	Average Data Quality
BASD	Ball Aerospace Systems Division
BOA	Bright Object Aperture
CASA	Center for Astrophysics & Space Astronomy
COS	Cosmic Origins Spectrograph
CU	University of Colorado
DEB	FUV Detector Electronics Box
DEC	Digital Event Counter in the FUV detector
DVA	FUV Detector Vacuum Assembly
ED	Engineering Diagnostic
FEC	Fast Event Counter in the FUV detector
FITS	Flexible Image Transport System
FUSE	Far Ultraviolet Spectroscopic Explorer
FUV	Far Ultraviolet
HST	Hubble Space Telescope
IDT	Instrument Development Team
INL	Integral Non-Linearity
LDCEDECA, B	Digital Event Counter for segments A and B
LDCEFECA, B	Front End Counter for segments A and B
LDCESDC1, 2	Science Data Counter 1 and 2
MDQ	Maximum Data Quality
NUV	Near Ultraviolet
OTA	Optical Telescope Assembly
P-flat	Pixel-to-pixel relative efficiency image
PHD	Pulse Height Distribution
PSA	Primary Science Aperture
QE	Quantum Efficiency
SM-4	Servicing Mission - 4
STScI	Space Telescope Science Institute
TDCA, B	Time-to-Digital Converter for segments A and B
TTAG	Refers to a data set acquired in time tag mode
UCB	University of California, Berkeley
1-D	One dimension
2-D	Two dimensions
RAS/Cal	Reflective Aberrated Simulator/Calibrator

1. INTRODUCTION & DOCUMENT ORGANIZATION

Welcome to AV-03 for COS, the Cosmic Origins Spectrograph for the Hubble Space Telescope. This document presents the final data products for COS observations, the calibration steps required to reduce flight COS data into the data product, and the preflight calibration requirements for the instrument. In addition, the reference files required for reducing the data are presented.

Before delving into this document the reader should be aware of a few things regarding the conventions used throughout this document and the flow of the information presented. First, the document starts with data products (§2), then outlines the required reference files (§3), presents flow of the data reduction and detailed algorithms for each step in the reduction process (§4), and concludes with ground calibration requirements (§5) and requirements for producing in-flight calibration reference files (§6). This top-down approach allows the reader to fully understand the flow of requirements from final data product back through to ground calibration. Admittedly, this can cause the reader some confusion, because topics are raised before they are fully explained, however, once the document is read in its entirety, all will become clear.

Generally speaking FUV time tag (TTAG) and image (ACCUM) related issues are presented first followed by NUV time tag and image issues, respectively. The reduction of COS flight data is broken up into two basic steps, whether it be FUV TTAG or ACCUM or NUV TTAG or ACCUM data. The raw data are first processed to remove detector effects, such as geometric distortion, and Doppler effects, and binned into an image. The spectrum is extracted from the image, corrected for intrinsic detector background and stray light, and flux calibrated. Therefore, there are six separate flows required to cover all the observational modes of COS. These flows are presented in flowchart form in section 4.1. Following the flowcharts are detailed algorithms for each step in the reduction process. If the reader has detailed questions regarding how data are reduced, section 4 is the place to look.

To minimize the trauma to the reader there are certain definitions that will aid in the reading process, especially early in the document. They are as follows:

- x and y refer to physical locations and can be in units of pixels, microns, or millimeters.
- P_x and P_y refer to the pixel values of a detected event in digital space, not physical space. This is pertinent only for the FUV detector where the plate scale of the detector is not constant in time or position. Therefore, a large part of section 4 is devoted to converting digital pixels into event locations in physical space.
- The indices i and j refer to the dispersion and cross-dispersion, respectively.

The presentations of the algorithms presented herein are designed for clarity for the reader, so that he or she may clearly understand what each individual step in the calibration process accomplishes. In certain cases it may be more suitable to combine steps to produce a more efficient computer code. Doing so is perfectly acceptable provided that the final result is functionally identical to what is described for each reduction step.

Finally, please recall that the FUV detector consists of two, identical segments. The implicit assumption throughout this document is that whenever the FUV data are discussed only a single segment is considered. However, what is good for one segment is also good for two segments, so all FUV data and FUV data reduction steps are applicable to both segments.

2. DATA PRODUCTS

2.1 INTRODUCTION

The data products are those data that are provided to the observer for a COS observation. They include such things as the raw data, corrected image in effective counts, corrected time tag list, and flux calibrated spectra to name a few. The data products are the same for each mode or type of observation, i.e. independent of grating/optic or aperture (PSA, BOA), or whether it is a science exposure, wavelength calibration, or flat field observation.

2.2 TIME TAG DATA

2.2.1 FUV Channel Data Products

2.2.1.1 Raw Data

The raw time tag data shall be a list of detected events in sequential order based on the time the event was detected. Each event shall consist of dispersion location (14 bits), cross dispersion location (10 bits), time word (31 bits), and pulse height value (5 bits). The raw data are the unprocessed detector data; therefore, they include source counts, sky background, intrinsic detector background, and stim pulses.

The data from the two segments are initially interleaved in the flight electronics. However, the raw data shall be separated based on segment and stored as separate files by the ground software.

2.2.1.2 Corrected Time Tag List

The time tag list is a fully corrected event list consisting of x, xd, y, t, ph, ε, q.

The x and y values are detector events corrected for thermal distortion, which is characterized by motion of the electronic stim centroids and geometric distortions, as determined by reference files generated during ground calibrations. Both these corrections will introduce floating-point pixels into the data set. For a description of the thermal and geometric distortions see sections 4.2 and 4.3 of this document.

The xd of the photon is the position of the event in non-integral pixels adjusted for orbital and heliocentric Doppler smearing, unlike x, which is the detected position of the photon. This allows the observer to form an image that is either in detector coordinates (x, y) or in wavelength space (xd, y), thereby allowing the observer to identify detector specific or wavelength dependent features. For example, if (x, y) are plotted a detector hot spot will be imaged, however, the spectrum will be blurred. On the other hand, if (xd,y) are plotted a detector hot spot will be blurred, but a monochromatic spectral line will be sharpened. The primary difference between x and xd is that Doppler smearing is accounted for in xd.

The t is the time for each event. The CS flight software inserts a time word into the time tag data stream every 0.032 seconds, so the arrival time for a given photon is only known to 0 to -0.032 seconds. The sequence of the photons in the time tag list for a given segment reflects the true order in which the photons were detected. However, it is possible that this ordering is not maintained between segments based on how the events are interleaved into the data stream.

The pulse height for a given photon is recorded in ph and is recorded as a 5-bit word in the flight data. The value of ph represents the charge extracted from the microchannel plate stack for that photon, or alternatively, the electron gain of the microchannel plate for an individual photon event.

ε is the sensitivity or weighting term for a photon event. It combines pixel-to-pixel response variations and live time correction. ε is derived from P-flats and knowledge of the detector live time (see sections 3.4, 4.6, and 4.7).

The term q represents the quality factor for a given event based on location of the detected event. The q assigned to a given event shall be determined from a bad active area list that will relate known detector blemishes with position. For example, if an event falls within the bounding box around a hot spot, that event will be assigned a value that indicates the event is likely from a hot spot. Each detector blemish will be assigned a

unique value to represent the severity and type of blemish. The q factors are assigned during ground processing of the flight data from a reference file.

2.2.1.3 Corrected Image

This detector image shall consist of a 16384 by 1024 image for each segment where the value in each pixel is in units of effective counts per second. In this case an effective count per second is the sum of all the ε factors associated with the counts in a given pixel divided by the actual length of the observation in seconds.

The image shall be formed from the corrected time tag data discussed above and using xd and y and standard threshold values for the pulse heights. Therefore, the image will be in wavelength space and corrected for Doppler smearing. The width of each pixel in the image shall be uniform in physical space.

The image shall not be corrected for dark rate, as this will be naturally included in any background subtraction.

2.2.1.4 Error Array

This data product is an error array of 16384 by 1024 pixels that reflects the errors in the corrected image at the pixel level. The errors are generated from the Poisson statistics from the gross counts and correcting the observed data for flat field and live time effects. The units shall be same as for the corrected image (effective counts per second).

2.2.1.5 Science Spectrum

The extracted science spectrum shall consist of wavelength (λ), gross count rate (GC), background count rate (BK), net count rate (N), flux (F), error bars (σ), maximum data quality (MDQ) in a resolution element, and the average data quality (ADQ). The wavelength refers to the central wavelength for a given spectral bin. All the bins are of equal width in physical space. The gross count rate is the count rate within a given wavelength bin of the spectrum, i.e. between the upper edge (XDISP pixel *d*) of the spectrum and the lower edge (XDISP pixel *c*) of the spectrum (see Figure 2.2-1). The background rate is the rate detected above and below the spectrum and averaged over a larger wavelength and scaled to the size of a spectral bin but with extents in the cross dispersion axis of pixel *a* to pixel *b* and pixel *e* to pixel *f* in Figure 2.2-1. The background regions are separated from the spectral region by half of a resolution element to insure that the spectral region does not contribute significantly to the background. The net count is the total number of events identified as source counts and is the gross counts minus the smoothed background counts and scaled by ε (see section 4.13 and equation

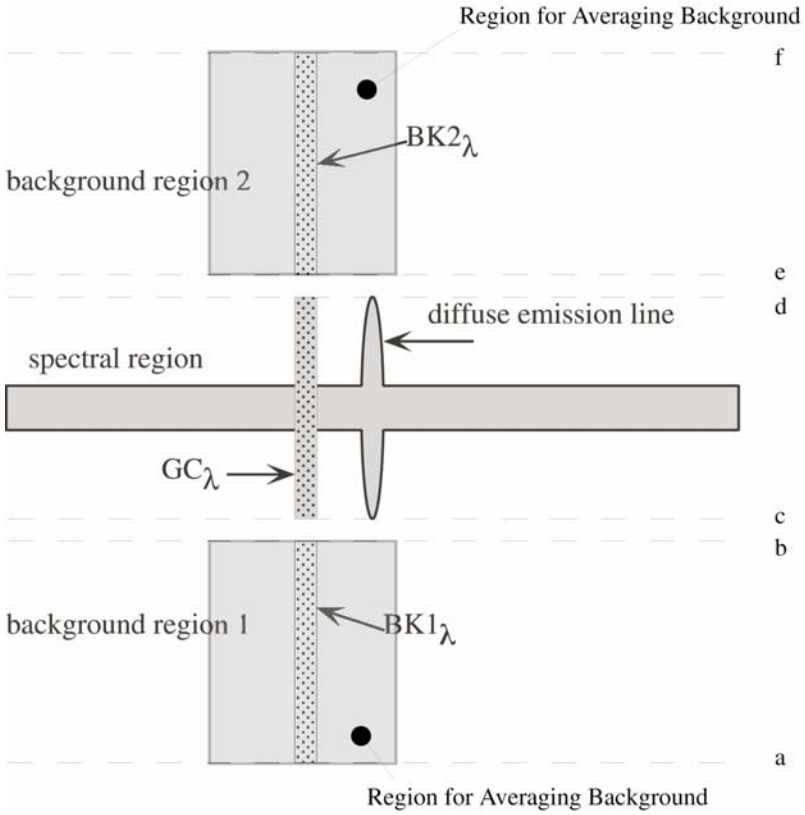

Figure 2.1-1: Schematic depicting the regions used for calculating the background contribution to the science spectrum.

4.13-6). Note that since the background is measured outside the image of the sky, any contaminating light from the sky will remain as part of the net counts.

The net count rate is then converted to flux via calibration reference files. The final error, σ, is in flux units and includes all sources of error as propagated through the reduction process. The maximum data quality (MDQ) is the maximum data quality flag of all the individual event quality flags within a given wavelength bin. The average data quality (ADQ) is the average of all individual event quality flags. With these two data quality flags it is possible to identify resolution elements that are near a detector blemish and the degree to which the data in those resolution elements are compromised.

In the case where multiple exposures are taken to support the FPSPLIT observing mode the individual spectra shall be weighted by the exposure specific fractional observing time and merged into a single file and provided to the observer (see section 4.16 for details).

2.2.2 NUV Channel Data Products

2.2.2.1 Raw Data

The raw time tag data shall be a list of detected events in sequential order based on time the event was detected. Each event shall consist of dispersion location (10 bits), cross dispersion location (10 bits), and time word (32 bits, of which 31 are significant).

2.2.2.2 Corrected Time Tag List

The corrected time tag list shall be a fully corrected event list consisting of x, xd, y, t, ε, q.

The x and y values are the locations of a single event. No geometric distortion corrections shall be made to the data.

The xd of the photon is the position of the event in non-integer pixels adjusted for orbital and heliocentric Doppler smearing, unlike the x position of the photon. This allows the observer to form an image that is either in detector coordinates (x, y) or in wavelength space (xd, y), thereby allowing the observer to identify detector specific or wavelength dependent features. For example, if (x, y) are plotted a detector hot spot will be imaged, however, the spectrum will be sharpened. On the other hand, if (xd,y) are plotted a detector hot spot will be blurred, but a monochromatic spectral line will be sharpened. The primary difference between x and xd is that Doppler smearing is accounted for in xd.

ε is the sensitivity or weighting term for a photon event. It combines pixel-to-pixel response variations and live time correction. ε is derived from P-flats and knowledge of the detector live time (see sections 3.4, 4.6, and 4.7).

The term q represents the quality factor for a given event based on location of the detected photon. The q assigned to a given event shall be determined from a bad active area list that will relate known detector blemishes with position. For example, if an event falls within the bounding box around a hot spot that event will be assigned a value that indicates the event is likely from a hot spot. Each detector blemish will be assigned a unique value to represent the severity and type of blemish. The q factors are assigned during ground processing of the flight data from a reference file.

2.2.2.3 Corrected Image

The detector image is formed from the time tag photon list. The image shall be 1024 X 1024 pixels and the values in each pixel shall be in effective counts per second. Effective counts per second is the sum of all the counts in a given pixel multiplied by the ε term for that pixel and divided by the length of the observation in seconds.

The image shall not be corrected for intrinsic background, as this will be naturally included in any background subtraction.

2.2.2.4 Error Array

This data product is an error array of 1024 by 1024 pixels that reflects the errors in the corrected image at the pixel level. The errors are generated from the Poisson statistics from the gross counts and correcting the observed data for flat field and live time effects. The units shall be same as for the corrected image (effective counts per second).

2.2.2.5 Science Spectra

The extracted science spectrum will consist of a table with columns wavelength (λ), gross count rate (GC), background count rate (BK), net count rate (N), flux (F), error bars (σ), the maximum data quality (MDQ) in a resolution element, and the average data quality (ADQ). The λ refers to the central wavelength for a given spectral bin. All the bins are of equal width in physical space. Gross count rate is the total number of counts within a given wavelength bin across the width of the spectrum. The extraction height is determined from in-flight observations of point source spectra and is a trade-off between better photometry (for larger heights) and better S/N (for smaller heights) and is set to avoid overlap of the spectral stripes.

The background rate is the average number of events detected on a portion of the NUV active area where the spectra do not fall. There is insufficient room between the spectra to estimate the background in a routine manner. For this reason the background is estimated using a region of the active area on either side of the spectral region on the detector. This region will remain fixed over the lifetime of the COS instrument. The net count rate is the total number of events identified as source counts and is the gross rate minus the average background rate per spectral bin. The net rate is converted to flux via calibration reference files. The final error, σ, is in flux units and includes all sources of error as propagated through the calibration process. The maximum data quality is maximum data quality flag of all the individual event quality flags within a given wavelength bin. The average data quality is the average of all individual event quality flags. With these two data quality flags it is possible to identify resolution elements that

are near a detector blemish and then how badly the data in those resolution elements are compromised.

In the case where multiple exposures are taken to support the FPSPLIT observing mode the individual spectra shall be weighted by the exposure specific fractional observing time and merged into a single file and provided to the observer (see section 4.16). Spectra acquired to cover different wavelength bands shall not be merged into a contiguous spectrum.

2.3 ACCUM DATA

2.3.1 FUV Channel Data Products

2.3.1.1 Raw Data

The raw data for an FUV ACCUM observation shall be a two dimensional array with a size of 16384 X 1024 pixels. Each pixel shall be capable of handling up to 65,536 counts (16 bits). Please note: the active area of the detector that contains the spectrum will be significantly smaller that 1024, per limitations in the onboard memory. However, the full 1024 pixels in the cross-dispersion direction shall be maintained to support the periodic adjustment of the spectrum in the cross-dispersion direction to mitigate gain degradation of the microchannel plates.

2.3.1.2 Corrected Image

The observer shall be provided with a corrected ACCUM image with a size of 16384 x 1024 pixels corrected for Doppler shifts, flat field response, and detector live time. The value in each pixel shall be in effective counts per second. Effective counts shall be computed by multiplying the ε term for a given pixel by the number of photons detected in that pixel. The actual length of the observation in seconds is then divided into the effective count image. Each image shall be corrected for thermal drift and geometrically corrected.

The image shall not be corrected for intrinsic background, as this will be naturally included in any background subtraction.

2.3.1.3 Error Array

This data product is an error array of 16384 by 1024 pixels that reflects the errors in the corrected image at the pixel level. The errors are generated from the Poisson statistics

from the gross counts and correcting the observed data for flat field and live time effects. The units shall be same as for the corrected image (effective counts per second).

2.3.1.4 Science Spectra

This is identical to the product discussed in section 2.2.1.4.

2.3.2 NUV Channel Data Products

2.3.2.1 Raw Data

The raw data for an NUV ACCUM observation shall be a two dimensional array with 1024 X 1024 pixels. Each pixel shall be capable of handling up to 65,536 counts (16 bits).

2.3.2.2 Corrected Image

This product shall be the 1024 X 1024 pixel image of the NUV detector corrected for Doppler shifts, flat field response, and detector live time. The corrected image shall not be distortion corrected.

The image shall not be corrected for intrinsic background, as this will be naturally included in any background subtraction.

2.3.2.3 Error Array

This data product is an error array of 1024 by 1024 pixels that reflects the errors in the corrected image at the pixel level. The errors are generated from the Poisson statistics from the gross counts and correcting the observed data for flat field and live time effects. The units shall be same as for the corrected image (effective counts per second).

2.3.2.4 Science Spectra

This is identical to the product discussed in section 2.2.2.4.

2.4 TA-1 IMAGE DATA

2.4.1 Raw Data

The raw image data for TA-1 mode observations shall consist of a 1024 X 1024 image. Each pixel shall be capable of handing 65,536 counts (16 bits).

2.4.2 Corrected Image

The calibrated image shall consist of a 1024 X 1024 image. Each pixel shall be capable of handing 65,536 counts (16 bits). The value in each pixel shall be in effective counts per second. Effective counts shall be computed by multiplying the ε term for a given pixel by the number of photons detected in that pixel. The actual length of the observation in seconds is then divided into the effective count image.

2.5 TARGET ACQUISITION IMAGE

For each observation a 2-D array shall be provided to the observer. This simple array, no bigger than 16 X 16, shall contain the measured net counts of the target for the appropriate detector at each of the dwell points for each phase of dispersed light target acquisition. Normal target acquisition can have multiple phases; therefore, the array may contain multiple data sets. For more information regarding target acquisition please refer to the Cosmic Origins Spectrograph Science Operations Requirements Document (OP-01).

2.6 FORMATS

All data files shall be provided in FITS formats.

3. REFERENCE FILES

3.1 WAVELENGTH CALIBRATIONS

3.1.1 Calibration Spectra

Calibration spectra shall be spectra of each calibration lamp and allowable current level for each spectroscopic mode of COS.

3.1.2 Wavelength Calibration Parameters

The wavelength calibration shall be a simple, low order polynomial expression that converts digital pixel to wavelength. The pixels in question are those in the geometrically correct space for the FUV detector and standard output pixels for the NUV detector. It shall be used for identifying the wavelengths associated with a given pixel in the image or converting an individual photon's wavelength back to pixels.

Each channel of the COS, FUV and NUV, and associated configurations, shall have a unique wavelength calibration solution.

3.2 SENSITIVITY CALIBRATIONS

The sensitivity calibrations shall be 1-D sensitivity versus wavelength curves generated by STScI for converting counts/sec into flux for a given instrument. The units shall therefore be (counts/sec/spectral bin)/(ergs/sec/cm^2/Å). The calibration curves for each observational mode shall be generated using observations of standard stars. Each channel in COS, whether it is an FUV or NUV channel, shall have a unique efficiency curve.

Deriving the sensitivity curves from a point source astrophysical target is adequate for generating high quality calibration data, as the qe variations of the photocathode across the detector, which will not be accounted for with a point source observation, are insensitive to position.

Each channel of the COS, FUV and NUV, and associated configurations shall have a unique sensitivity calibration.

3.3 SPECTRAL EXTRACTION TEMPLATES

This reference file shall provide the coefficients of a linear function that describes the location of the center of each spectrum in the cross dispersion direction versus the dispersion pixel value. In addition, this file shall contain a distance, in pixels, from the linear function that encompasses the full width of the spectrum (see Figure 4.13-1).

Each channel of the COS, FUV and NUV, and associated configurations shall have a unique extraction template.

3.4 FLAT FIELD DATA & DERIVATIVES

This shall consist of the raw data along with the computed L-fits and P-flats. Flat field data for each detector shall be derived using onboard calibration lamps. These lamps naturally have wavelength dependent structure that eliminates the possibility of uniform illumination. The raw data will not be a single exposure, but a combination of several subexposures, such as FPSPLITS, non-standard OSM1 positions (both rotary and linear). This strategy will suppress the fine scale structure in the lamp spectrum while preserving the wavelength and illumination geometry. Thus, a multi-step process is used to extract the pixel-to-pixel response of the detectors.

The first step produces an L-fit. An L-fit is a two-dimensional function that follows the low frequency modulation of the spectrum. It is typically formed by fitting a spline

functional to the data or by using a rolling average to create the low frequency model. (see Figure 3.4-1). The current baseline is to use an 11^{th} order polynomial as the function form of the L-fit. This is based on a preliminary analysis of the measured INL of the flight detector.

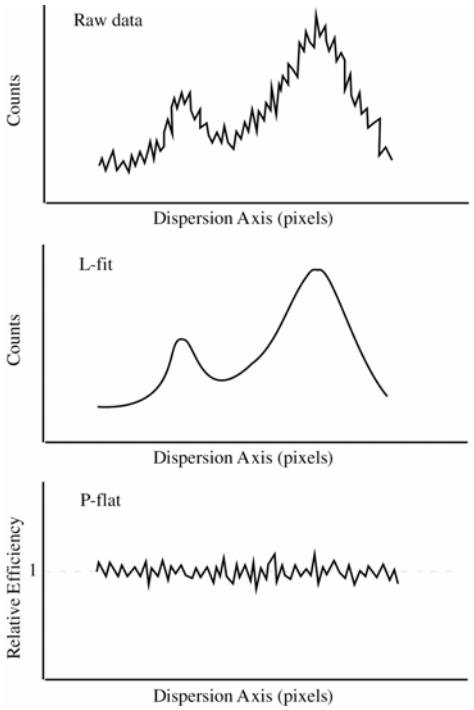

Figure 3.4-1: Derivation of L-fits and P-flats. Upper panel represents the raw data acquired using the onboard flat field lamp. Middle panel shows the L-fit and the bottom panel shows the P-flat, the raw data divided by the L-fit.

The second step produces a P-flat. A P-flat is produced by dividing the raw data by the L-fit, thus removing the low frequency component from the data and leaving the high frequency, pixel-to-pixel response of the detector with an average of 1 (see Figure 3.4-1).

There shall be three P-flats, one for each segment of the FUV detector and one for the NUV detector.

3.5 DATA QUALITY REFERENCE TABLES

These data shall consist of a table with lx, ly, dx, dy, feature type, and q. lx and ly are the coordinates in digital pixels in geometrically correct space of the lower left edge of a bounding box of dx width in the dispersion direction and dy width in the cross-dispersion direction. The feature type describes the type of detector blemish enclosed within the bounding box and q is the quality value assigned to all events detected within the bound

box. The types of detector blemishes shall include such features as hot spots, dead zones (type I and II, as defined by the *FUSE* Data Handbook; Oegerle, Murphy, & Kriss 2000), edge effects, grid lines (if they exist), and any other errors that are constant in time and location on the detector.

There shall be three data quality reference tables, one for each segment of the FUV detector and one for the NUV detector. These tables shall require periodic updating as the microchannel plates age (about every 3 months).

Table 3.5
Binary Data Quality Flag Values

Flag	Condition
00000000	No anomalous condition noted
00000001	TBD
00000010	Grid shadow >TBD % variation above the flat field response
00000100	Live-time discrepancy – SDC1/DEC/FEC differ by more than 3σ from average count rate
00001000	Dead spot
00010000	Hot spot
00100000	Anomalous pulse height distribution
01000000	Time segment excluded in data
10000000	Data fill, Telemetry drop out

3.6 DETECTOR LIVE TIME CALIBRATIONS

These data shall consist of the measured data and the reduced calibration data, which shall relate the live time of the detector to the output count rate of the detector. Please refer to section 4.6 for more details on how the live time for each detector is computed.

3.6.1 FUV Detector

The raw data for each segment will consist of the global input count rate to the time to digital converters (TDC) as measured by the fast event counters (LDCEFECA and LDCEFECB) versus the observed output count rate from the TDCs as measured by the digital event counters (LDCEDECA and LDCEDECB). The reduced data will simply relate the LDCEDECA and LDCEDECB values to a live time correction factor.

A second set of data is necessary to fully understand the live time of the FUV detector subsystem. This will include the observed output count rate from the time to digital converters as measured by the digital event counters (LDCEDECA and LDCEDECB)

and the output rates from the "round robin", the science data rate monitors (LDCESDC1 and LDCESDC2). Please refer to section 4.6 for a more thorough description of the FUV live time.

3.6.2 NUV Detector

The live time calibration data shall consist of output count rate versus live time.

3.7 FUV DETECTOR DISTORTION MAP

This shall include the slit pattern data and pinhole data acquired during detector calibration along with the distortion map for each axis as computed using the two data sets. Please refer to section 4.4 for details on how geometric distortion is measured and corrected.

3.8 FUV DETECTOR BASELINE REFERENCE DATA

These data shall include quantities such as the nominal stim locations, pulse height threshold levels, etc. Please see section 4.3 for details on the baseline reference frame.

3.9 FORMATS

All reference files shall be maintained as FITS formats.

4. CALIBRATION OF COS FLIGHT DATA

4.1 INTRODUCTION

The calibration of COS flight data shall follow specific steps to maintain the integrity of the data. For clarity these steps are first presented as flowcharts and then each step is discussed individually in more detail in the subsequent sections.

4.1.1 FUV & NUV Calibration Flows

The flowcharts for the FUV and NUV data follow a similar methodology. The raw data, in either TTAG or ACCUM, are first processed to remove detector effects and observational effects associated with the wavelength scale, e.g. Doppler corrections. The spectrum is extracted from a 2-D image, corrected for intrinsic detector background and stray light, and flux calibrated. Figures 4.1-2 through -4 show the processes associated with the FUV data and Figures 4.1-5 through -7 present the similar processes for the NUV data. Figure 4.1-8 shows the processing flow for an image acquired with the TA-1 mode.

The flowcharts in Figures 4.1-2 through 4.1-8 use the symbols presented in Figures 4.1-1 to represent processes, inputs and outputs, and reference files.

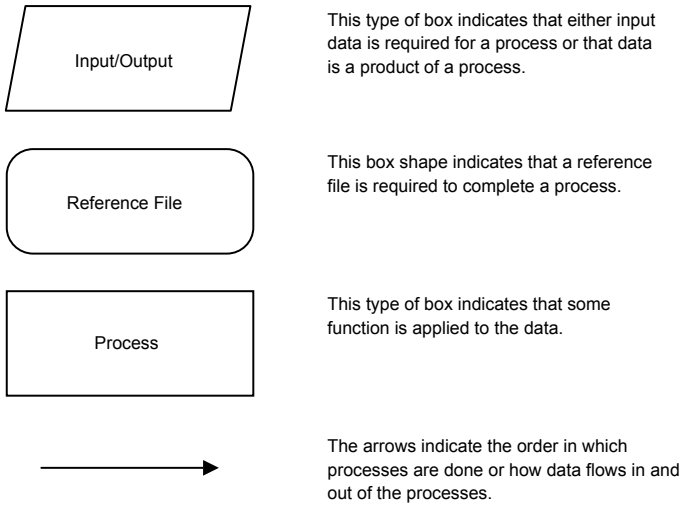

Figure 4.1-1: Flowchart Key

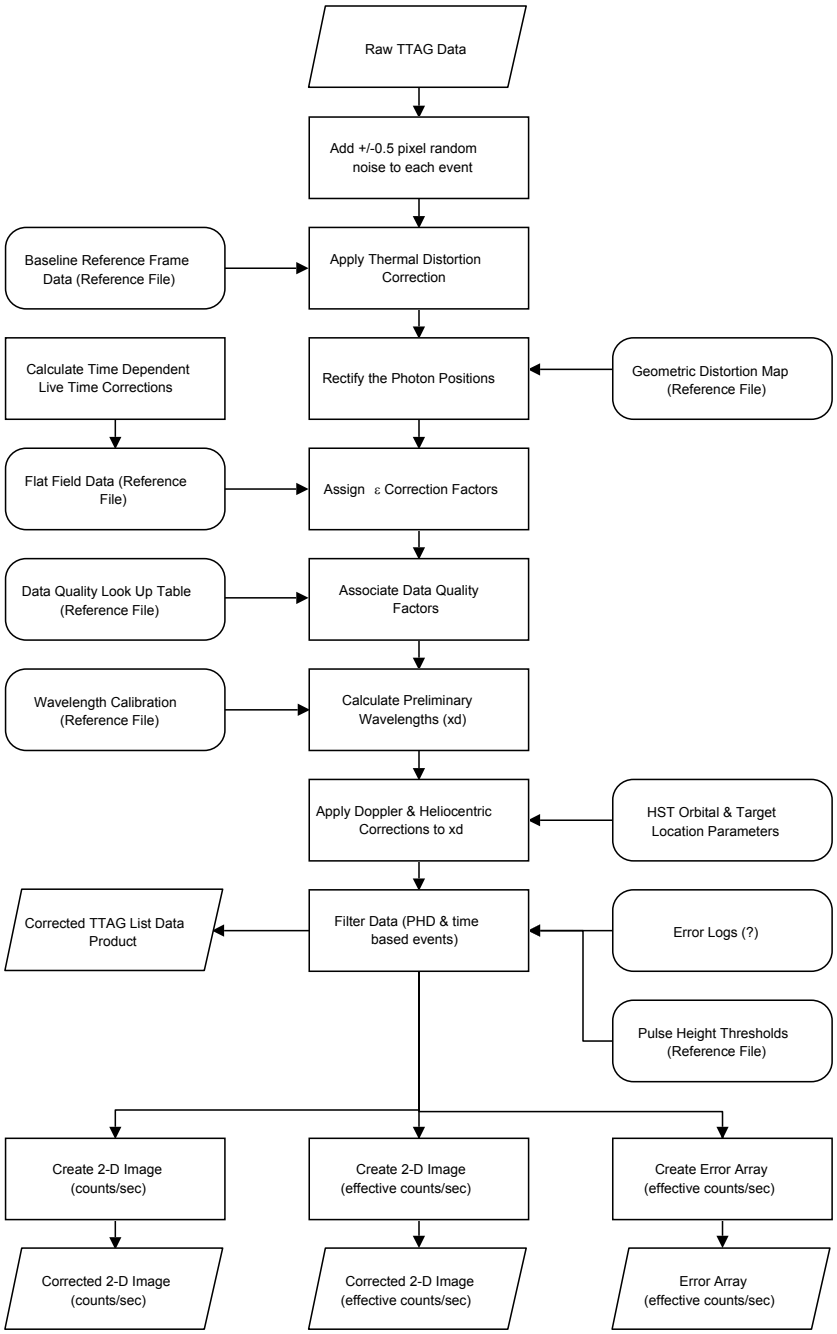

Figure 4.1-2: This flowchart depicts how raw FUV TTAG data are processed to produce the corrected time-tag, effective counts/second image, and counts/second image data products necessary for extraction of the science spectrum.

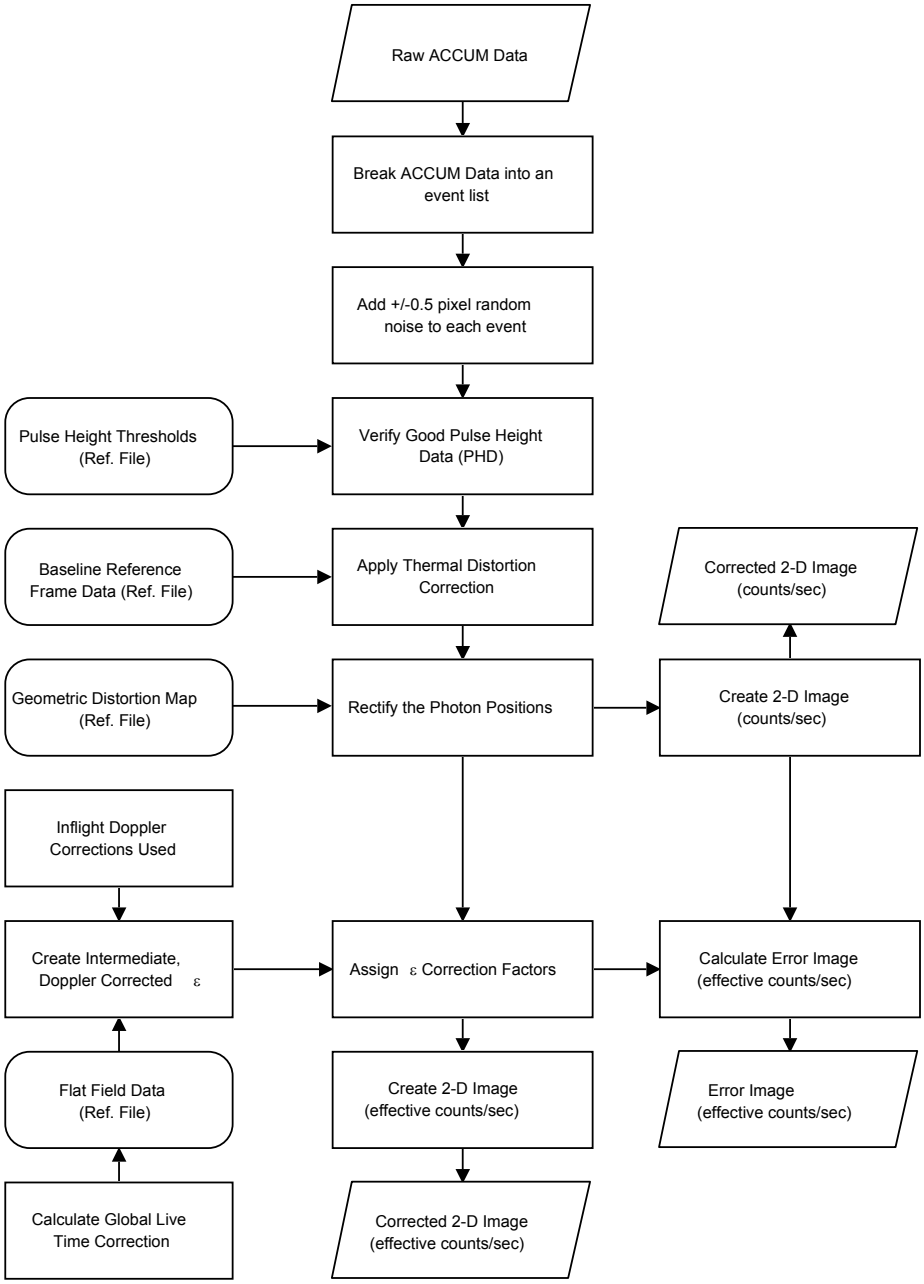

Figure 4.1-3: This flowchart depicts how raw FUV ACCUM data are processed to produce the effective counts/second image and counts/second image data products necessary for extraction of the science spectrum.

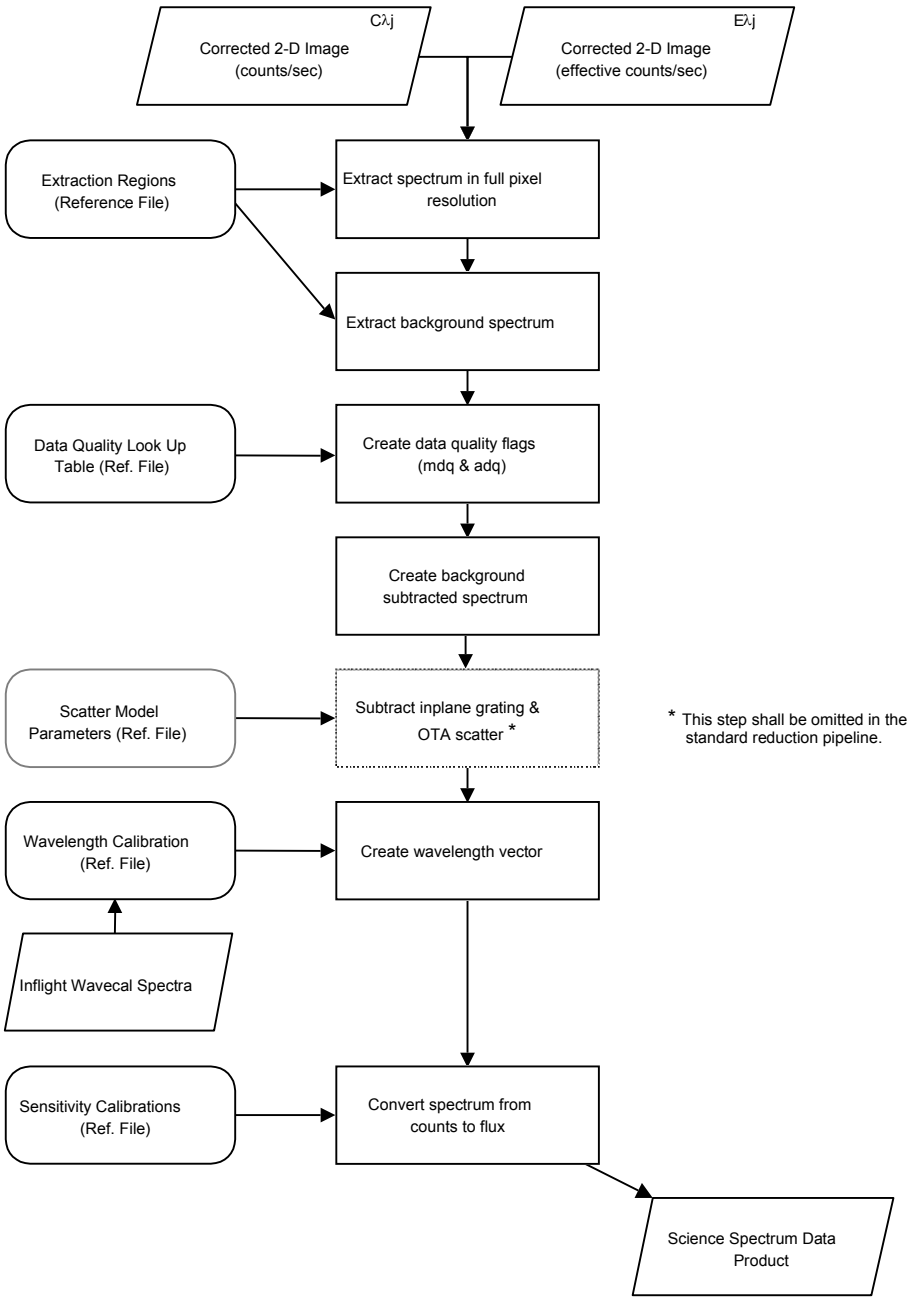

Figure 4.1-4: This flowchart depicts how the FUV spectral data are extracted and processed to produce the final calibrated spectrum for a single exposure.

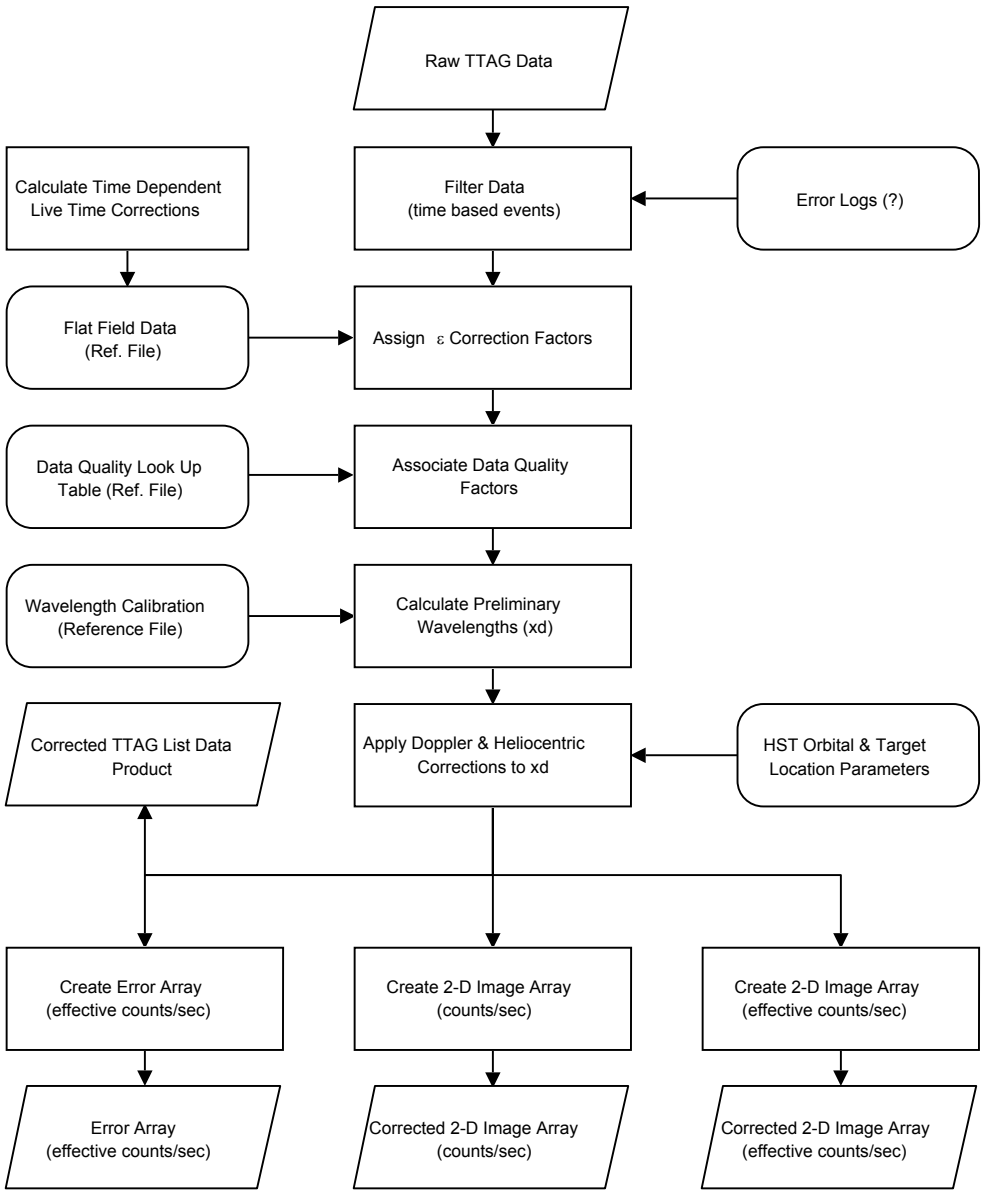

Figure 4.1-5: This flowchart depicts how raw NUV TTAG data are processed to produce the corrected time-tag, effective counts/second image, and counts/second image data products necessary for extraction of the science spectrum.

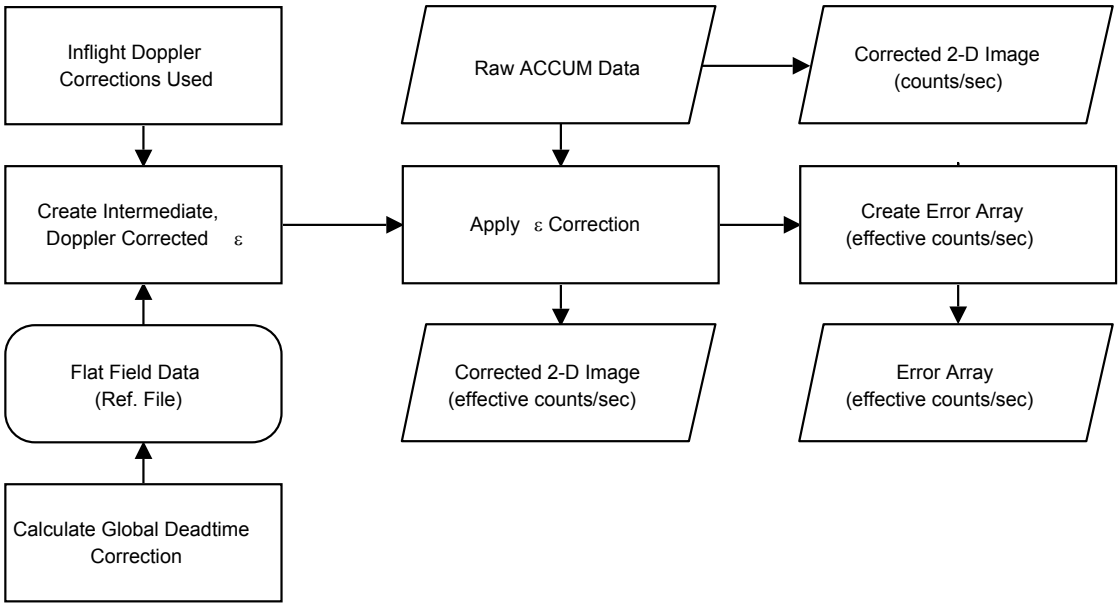

Figure 4.1-6: This flowchart depicts how raw NUV ACCUM data are processed to produce the effective counts/second image and counts/second image data products necessary for extraction of the science spectrum.

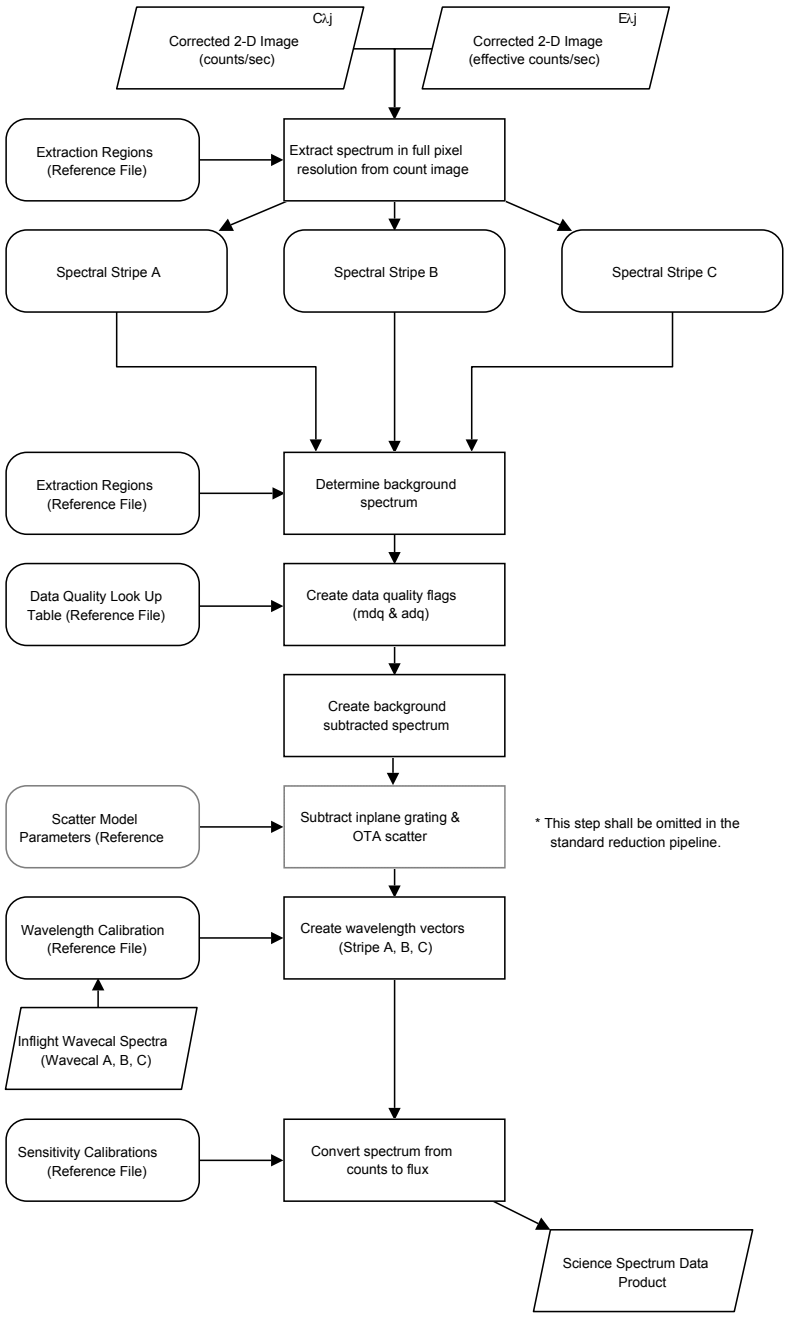

Figure 4.1-7: This flowchart depicts how the NUV spectral data are extracted and processed to produce the final calibrated spectrum for a single exposure.

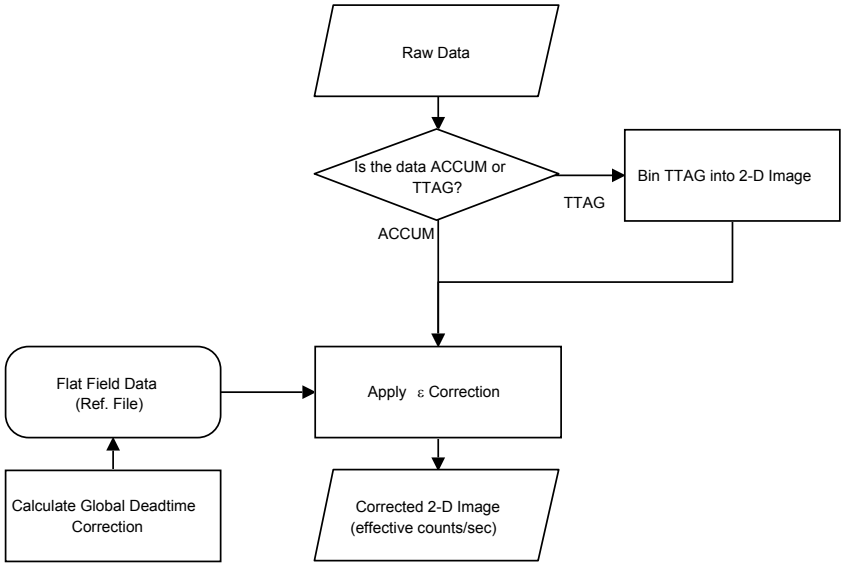

Figure 4.1-8: This flowchart depicts how the NUV TA-1 image data are extracted and processed to produce the final calibrated image for a single exposure.

4.2 ALIASING EFFECTS & COMPENSATION

This section relates only to the FUV detector and the data generated by it. The inclusion of this section is necessitated by the analog nature of the detector. The issue here is that, as is described in detail in section 4.3, the FUV data will be rescaled to compensate for changes in the pixel scale induced by thermal variations in the detector anode and electronics. This rescaling effectively stretches or compresses the positional data. In doing so it is possible to introduce a "gap" in the data, entire columns or rows with no data (also known as the aliasing effect). An example of this effect is shown in figure 4.2-1.

There are several ways of compensating for aliasing effects, including geometric resampling (e.g. the IDL routine FREBIN), using bilinear interpolation to calculate the expected data at a given location, and dithering of the digital data, where a uniformly distributed value Δx, where $-0.5 < \Delta x \leq +0.5$ pixels, is added to the digital data prior to assigning each count to the nearest neighbor bin in the geometrically correct space. Any of these solutions is probably acceptable, however, there are certain practical considerations that make using the dithering technique the most preferable. First, dithering is the only option available for TTAG data. Second, it is highly advantageous for the reduction algorithms to be as similar as possible to minimize potential differences in the spectra between calibrated TTAG and ACCUM data. This also minimizes the amount of software needed and can save significant amounts of time and money in development and maintenance of the computer code.

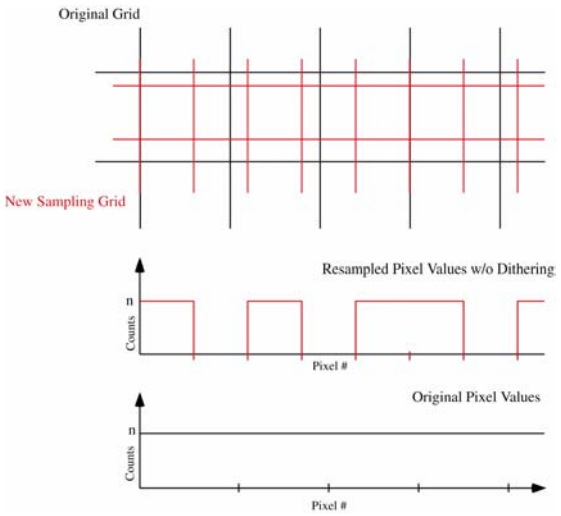

Figure 4.2-1: This figure schematically shows how assigning counts to the nearest neighbor bin in an array with a new grid can introduce gaps in the data. This effect is

known as “aliasing” and is corrected by dithering, geometric resampling, or bilinear interpolation.

The question then remains, how can dithering be applied to an ACCUM image. The answer is that the ACCUM image shall be broken up into an event list of N items, the total number of events in the ACCUM image. For example, consider pixel i,j with n events. Pixel i,j shall be converted to an event list by generating 2*n uniformly distributed random numbers ranging from greater than –0.5 to less than or equal to +0.5. These random values shall be added to the pixel values i and j. In doing so n events will be created that are uniformly distributed over the pixel. In addition, a constant time word shall be added to each event. The exact nature of the time word, e.g. the beginning, middle, or end of the exposure, shall be left up to the Space Telescope Science Institute’s discretion.

After the ACCUM image is converted to an event list the algorithms for compensating for the changes in the plate scale and geometric correction shall be identical to those used for TTAG.

4.3 THE FUV BASELINE REFERENCE FRAME

4.3.1 TTAG Data

The FUV detector pixelization of a photon event changes with temperature. Details of this effect are documented in memos by Geoff Gaines at UCB (FUSE-UCB-014) and Erik Wilkinson at CU (COS-11-0011). Two effects are known to change the plate scale of the detector: temperature dependence of the dielectric constant of the anode substrate in the DVA and temperature dependence of the integrating capacitor in the DEB digitizers. The positions of the electronic stims are used to monitor changes in the plate scale of the detector. The anode introduces a stretch in the plate scale that moves the locations of the electronic stims by ~±4 pixels/˚C. The integrating capacitor introduces a stretch (~1.5 pixels/˚C) and a small offset in the center of the image (0.3 pixels/˚C) in the dispersion direction.

The change in pixel scale induced by thermal variations in the anode substrate shall be monitored and corrected by tracking the locations of the electronic stim pulses, which are fixed in physical space. The detector thermal environment has been engineered to be thermally stable with variations not more than +/- 0.3 ˚C/orbit at the DVA and ±2.5 ˚C/orbit at the DEB. The current estimate of the magnitude of the thermally induced change in pixel scale is <±5 pixels/˚C at the stim locations. The center of the anode experiences less than a 1 pixel shift. Current understanding of the thermal subsystem performance indicates that changes in pixel scale will be small. However, differences

between the thermal environment during ground testing and flight could be substantial, thereby necessitating that either the flight data or the calibration data are manipulated into a common thermal reference frame. This common reference frame is referred to as the Baseline Reference Frame and shall be defined by centroids of the electronic stim pin in pixels.

The stretch of the pixel scale is, as far as is known at this time, linear. The expression for mapping the position of any detected photon at an arbitrary pixel scale to its physical position in the Baseline Reference Frame using the electronic stim locations is derived below.

Finally, the thermal distortion is a time dependent effect, therefore, the correction is also time dependent. For this reason, TTAG exposures shall be broken up into 10-minute subsets. Each subset shall be individually corrected back to the Baseline Reference Frame.

Definitions:

1) X – physical location of a detected photon in microns (NOT pixel value).
2) S_{x1} – the centroid of the low value pixel electronic stim in the dispersion direction at temperature T_1 (*calibration constant*).
3) S_{x2} – the centroid of the high pixel value electronics stim in the dispersion direction at temperature T_1 (*calibration constant*).
4) S'_{x1} – the centroid of the low pixel value electronic stim in the dispersion direction at temperature T_2.
5) S'_{x2} – the centroid of the high pixel value electronic stim in the dispersion direction at temperature T_2.
6) a – the X offset in microns at T_1 .
7) a' – the X offset in microns at T_2.
8) b – the pixel scale in microns/pixel at T_1.
9) b' – the pixel scale in microns/pixel at T_2.
10) P_x – pixel value of the photon at T_1.
11) P'_x – pixel value of the photon at T_2.

At T_1 the position X of a photon is described by....

$$X = a + bP_x \qquad \text{Eqn. 4.3-1}$$

and at T2 by;

$$X' = a' + b' P'_x \qquad \text{Eqn. 4.3-2}$$

The electronic stims remain fixed in physical space, so X = X' for an electronic stim. Therefore, we can solve for a and b at all times using the electronic stim locations. The solution goes as follows:

At X = X' we have for each electronic stim location…

$$a + bS_{x1} = a' + b' S'_{x1} \qquad \text{Eqn. 4.3-3}$$

$$a + bS_{x2} = a' + b' S'_{x2} \qquad \text{Eqn. 4.3-4}$$

so,

$$a' = a + bS_{x1} - b'S'_{x1} \qquad \text{Eqn. 4.3-5}$$

$$b' = b\frac{S_{x2} - S_{x1}}{S'_{x2} - S'_{x1}} \qquad \text{Eqn. 4.3-6}$$

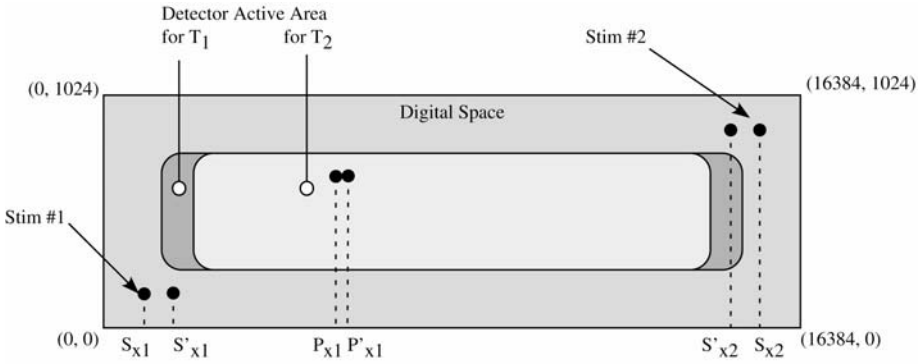

Figure 4.1-1: Schematic representation of the locations of the electronic stims and the associated change in plate scale of the detector active area.

Given the centroid of the electronic stims at any given time, any photon can be mapped to a fixed position in physical space using equation 4.3-1. Combining equations 4.3-2, -5, and –6 results in equation 4.3-7.

$$X' = a + b\left[S_{x1} + \frac{(S_{x2} - S_{x1})}{(S'_{x2} - S'_{x1})}\left(P'_x - S'_{x1}\right)\right] \qquad \text{Eqn. 4.3-7}$$

X' must now be converted back into units of pixels at temperature T_1 ($X' \equiv X$), so equating equation 4.3-7 to equation 4.3-1 and solving for P_x we get equation 4.3-8, which is the pixel value for a photon detected at temperature T_2 in the pixel scale at T_1.

$$P_x(P_x^{'}) = S_{x1} + \left(P_x^{'} - S_{x1}^{'}\right)\frac{\left(S_{x2} - S_{x1}\right)}{\left(S_{x2}^{'} - S_{x1}^{'}\right)} \qquad \text{Eqn: 4.3-8}$$

An identical expression for the cross dispersion axis (Y) is also applicable, however, the larger pixels in the cross dispersion direction may make it unnecessary to correct for thermal distortions (see equation 4.3-9).

$$P_y(P_y^{'}) = S_{y1} + \left(P_y^{'} - S_{y1}^{'}\right)\frac{\left(S_{y2} - S_{y1}\right)}{\left(S_{y2}^{'} - S_{y1}^{'}\right)} \qquad \text{Eqn: 4.3-9}$$

4.3.2 ACCUM Data

FUV ACCUM data, like TTAG data, shall be corrected for thermally induced changes in the detector plate scale. The corrections shall be identical to those used to correct the TTAG data. Unlike the TTAG, there is no need to break the ACCUM event list into time segments, although since a constant time is associated with each ACCUM event, there should be no need to alter the software between TTAG and ACCUM corrections.

Note that the electronic stims for an ACCUM image are stored as separate files and shall also be corrected for the thermal distortion.

Calibration Constants		
Left hand stim location, DISP direction	S_{x1}	
Left hand stim location, X-DISP direction	S_{y1}	
Right hand stim location, DISP direction	S_{x2}	
Right hand stim location, X-DISP direction	S_{y2}	

4.4 CORRECTING FOR GEOMETRIC DISTORTIONS

The object of correcting for geometric distortions is to produce a geometrically uniform image with pixels of equal size from an image where the pixel size in physical space varies across the detector.

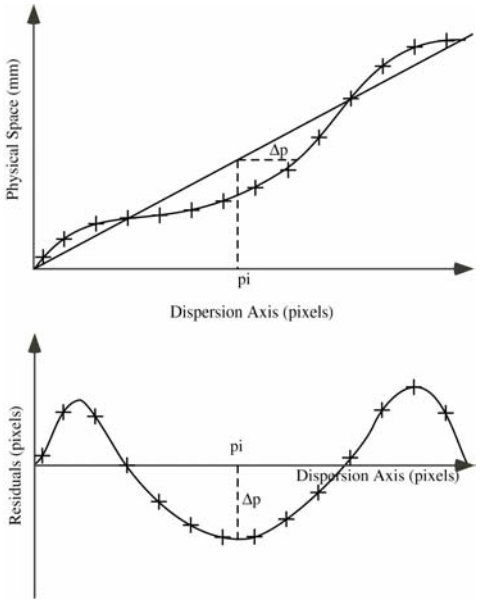

Figure 4.4-1: Upper panel shows the measured locations of the slits (crosses) versus their actual locations with a best-fit line through the data. The lower panel shows the residuals (INL) that are applied to the data to correct for the geometric distortion per Equation 4.4-1.

4.4.1 FUV Data

FUV data, whether ACCUM or TTAG, shall be corrected for integral non-linearity (INL). Integral non-linearity is defined to be variations in the plate scale of the detector that occur on scales ≥1 mm. The INL is calibrated at the detector level and this calibration data is carried forward throughout the mission lifetime to correct for distortion. The INL is calibrated by comparing the actual location versus measured location of either a slit pattern (for the dispersion axis) or a pinhole pattern (for the cross dispersion axis). The pattern is generated by placing a metal sheet with precision air slits, or pinholes, directly onto the top microchannel plate of the detector and illuminating the detector with photons. The slits are 25 X 500 microns and separated by 200μm in the dispersion direction. The pinholes are 10μm diameter on a 0.5mm grid. The slits or pinholes are illuminated with UV radiation and the resulting image is recorded.

The data are then analyzed by measuring the position of each slit in the dispersion and cross dispersion directions, fitting linear functions to the data, and subtracting the best fit line from the measured positions to form the residuals. The plot of residuals versus dispersion axis pixel is a measurement of the INL. Figure 4.4-1 shows what the INL might look like.

In general terms, correcting the data for the INL means that the data positions are adjusted so that the residuals are zero.

4.4.1.1 TTAG Data

Correcting TTAG data for INL is a simple process. The dispersion coordinate of each photon event is adjusted by the measured INL for events at that location. For events that fall between two slit images a linear fit between the points will be sufficient for calculating the INL, however, any other appropriate functional form shall be acceptable. (Figure 4.4-2) schematically depicts this process and equation 4.4-1 explicitly defines the procedure.

$$P_x^{'} = P_x - INL(P_x) \qquad \text{Eqn. 4.4-1}$$

In the cross-dispersion direction an identical process shall be used. However, given the lower resolution and coarser pixel scale in the cross-dispersion direction the magnitude of the INL will be significantly smaller compared to the dispersion direction.

The INL has no cross coupling between axes, so each axis may be treated independently.

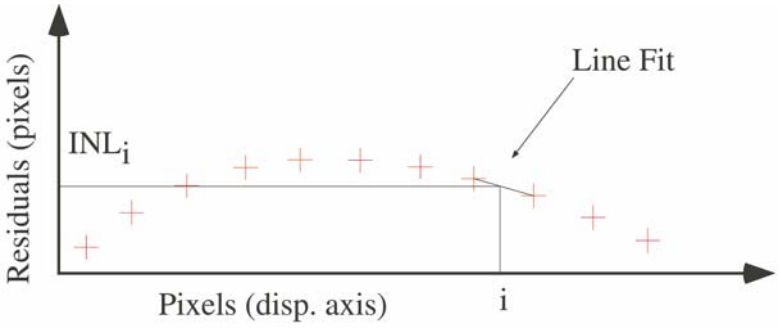

Figure 4.4-2: This figure depicts how a line between the residuals for two slits is used to interpolate the amount of integral non-linearity (INL_I) for pixel i. Any other appropriate functional form for interpolating between points shall be acceptable.

4.4.1.2 ACCUM Data

The ACCUM data shall be corrected for INL in a manner identical to that used for the TTAG data (see section 4.4.1.1).

4.4.2 NUV Data

No corrections for geometric distortions are required for any NUV data.

4.4.3 MEASURED INTEGRAL NON-LINEARITY

Figures 4.4.1 and 4.4.2 show schematic representations of integral non-linearity and how it is used to correct for geometric distortions. The integral non-linearity of the flight detector has a completely different shape compared to Figure 4.4.1. Figure 4.4.3 presents the INL measured for segment A of the FUV flight detector. As described in sections 3.7 and 4.4.1 the INL is characterized using images of slits and pinholes acquired during detector development. The INL files along with the slit and pinhole images are provided as reference files.

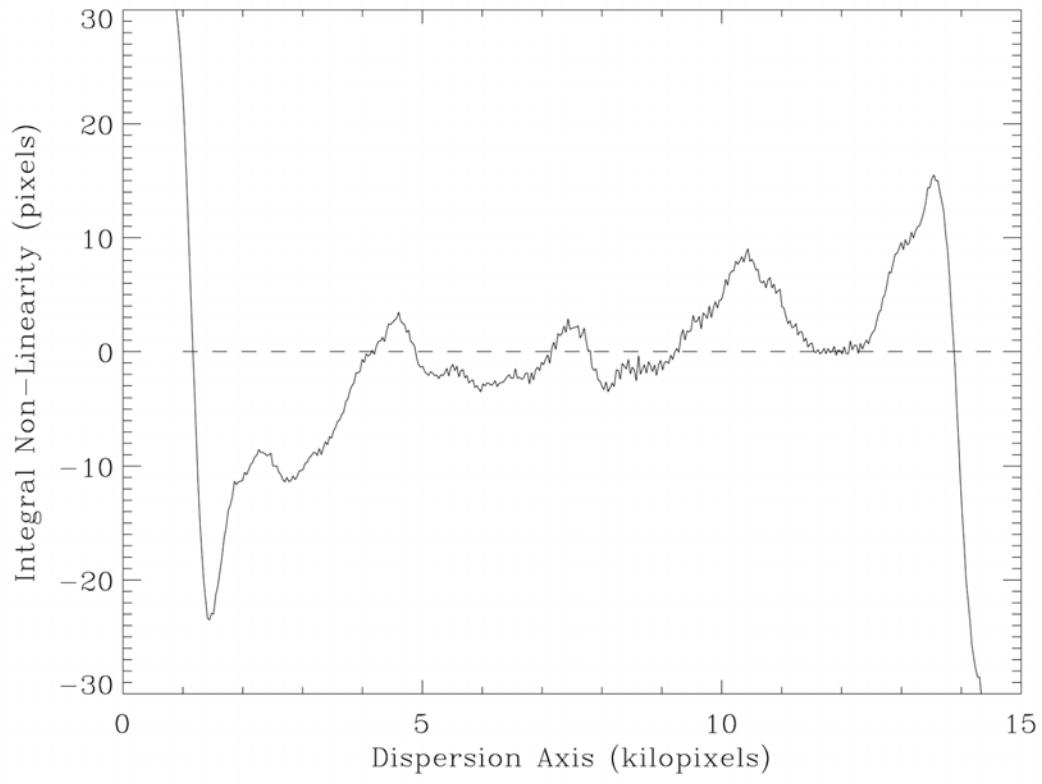

Figure 4.4-3: Measured integral non-linearity for segment A of the FUV flight detector.

4.5 FLAT FIELDS

The three flat field data sets for the NUV and FUV detectors shall be maintained as images. The two FUV flat field images shall be 16384 X 1024 pixels and the NUV flat field image shall be 1024 X 1024 pixels. Derivation of the flat field data is discussed in section 5 of this document.

4.5.1 TTAG Data

The flat field response for a photon event is based on the location of the event on the MCP active area. In the case of NUV TTAG data there is a one-to-one correlation between an event's location on the MCP active area, digitized location in pixels, and flat field pixels.

FUV data, on the other hand, must first be corrected for thermal and geometric distortions to determine the physical location of the event on the MCP active area. As discussed earlier, the result of these corrections is that for TTAG data a photon's location is expressed as two floating-point numbers (P_x, and P_y) in units of pixels. The correct flat field response for a photon event shall be the response of the pixel in the flat field image identified where $P_{ix}-1/2 \le P_x < P_{ix}+1/2$ and $P_{iy}-1/2 \le P_y < P_{iy}+1/2$. For example, the flat field response for a photon detected at (9248.239, 784.689) will be located at (9248, 785) in the flat field array.

4.5.2 ACCUM Data

ACCUM data are maintained in an image array format. Therefore, there is a one-to-one correlation between the pixels in the data and the pixels in the flat field.

The onboard Doppler correction of the data necessitates that the flat fields are handled differently than for the TTAG data. The onboard Doppler correction maintains a constant wavelength scale as the spectrum moves across the detector active area due to Doppler shifts. Therefore, the flat field for a given wavelength pixel is actually the result of multiple flat fields, each being the baseline flat field offset in the dispersion direction by a single pixel.

Therefore, for ACCUM images an interim flat field shall be produced that is the average of exposure time weighted and offset flat field images corrected for the in-flight Doppler correction. This interim flat field shall be used in the reduction of all ACCUM images, whether they are FUV or NUV. Mathematically, this can be expressed by equation 4.5-1.

$$iFF = \frac{FF_0 \cdot \Delta t_0 + FF_1 \cdot \Delta t_1 + FF_2 \cdot \Delta t_2 \ldots + FF_n \cdot \Delta t_n}{t_{\mathrm{exp}osure}} \qquad \text{Eqn. 4.5-1}$$

where

iFF is the intermediate flat field array.
FF_i is the flat field image array.

The subscript indicates the number of columns the FF has been shifted, positive values are for shifts to the right, negative values for the shifts to the left.

n is the maximum number of pixels the onboard Doppler correction adjusted the data during the acquisition.

Δt_i is the time of the sub-exposure, where the sub-exposure is defined as the length of time for a Doppler step in the COS flight software.

$t_{exposure}$ is the total exposure time.

Table 4.5-1

Calibration Constants		
Flat field image	**FF**	
Intermediate flat field image	**iFF**	
Sub-exposure time for Doppler step.	$\mathbf{\Delta t_i}$	
Exposure time	$\mathbf{t_{exp.}}$	
Magnitude of Doppler shift (pixels)	$\mathbf{D_{mag}}$	
Time of zero Doppler shift	**t0**	
Orbital period of HST	$\mathbf{T_{HST}}$	

4.6 LIVE TIME CORRECTIONS

A component of the flat field correction is the live time correction associated with the detector electronics. The live time correction shall be determined differently depending upon the observing mode in which the data were acquired, as discussed below.

4.6.1 How Live Time is Determined

Live time is an important aspect of detector performance. This section outlines how live time is computed for each of the detectors onboard COS. In general terms, live time is the ratio of the number of events counted by the detector electronics compared to the number of events entering the detector electronics and thus is a measurement of the efficiency of a photon counting detector's electronics in processing data. Dead time, another common term for describing the efficiency of electronic system, is one minus the live time.

The FUV detector subassembly is really two entirely separate detectors up until the data streams are merged in the DEB. As such, the live time has two components; the live time associated with the segment specific electronics (dominated by the time to digital converters) and the live time associated with the electronics that merge the data stream (referred to as "round robin").

In the case of the FUV detector there are three places where live time is introduced into the system; the fast amplifiers, the time-to-digital converter, and finally the round robin, which is common to both detectors (See figure 4.6-1). This means that the live time between segments will likely be different based on the distribution of flux across the detector.

There are three counters that monitor the count rates throughout the processing and can be used to monitor and correct for the live time. The first are the fast event counters (LDCEFECA & LDCEFECB) that report output rate of the fast amplifiers. The digital event counters (LDCEDECA & LDCEDECB) report the output rate of the time-to-digital converters. Finally, the science data counters (LDCESDC1 and LDCESDC2) report the output rate of the round robin.

The dominant source of live time is the time-to-digital converters. At count rates less than 50 kHz the fast amplifiers and round robin circuitry introduce ~ 98% live time, which is still dominated by the fast amplifiers. On the other hand, the time-to-digital converters introduce ~75% live time at 50 kHz.

Based on this understanding, the following assumptions shall be used in determining the live time for the FUV detector:

1. The round robin does not introduce significant live time at count rates below 50 kHz, a rate 25% greater than the maximum global rate for the detector.
2. The FEC rates are dominated by full gain photon events and not low gain noise events.

With respect to item 2, the FEC shall be thought of as reporting the input photon rate with a small correction for live time. However, the FEC reports *all* events that trigger the fast amplifiers. The inputs to the FEC have very low thresholds, thus they report low gain events as well as photon events with higher gain. This is done to provide insight into the performance of the microchannel plates, such as reporting low gain hot spots. In instances where significant noise from the microchannel plates is introduced into the fast amplifiers, the derived photon rate computed entering the fast amplifiers will be incorrect. This can lead to inaccuracy in the photometric calibration of the data. Comparing the FEC rate computed using the DEC rate with the FEC rate reported in the flight telemetry identifies this condition. The accuracy of the photometry may be recovered through analysis and reprocessing of the data, albeit outside of the pipeline processing and depends upon the nature of the noise component.

The NUV detector has a single data pipeline, thus the live time can be effectively characterized by the output count rate and an associated calibration curve which relates live time to output count rate.

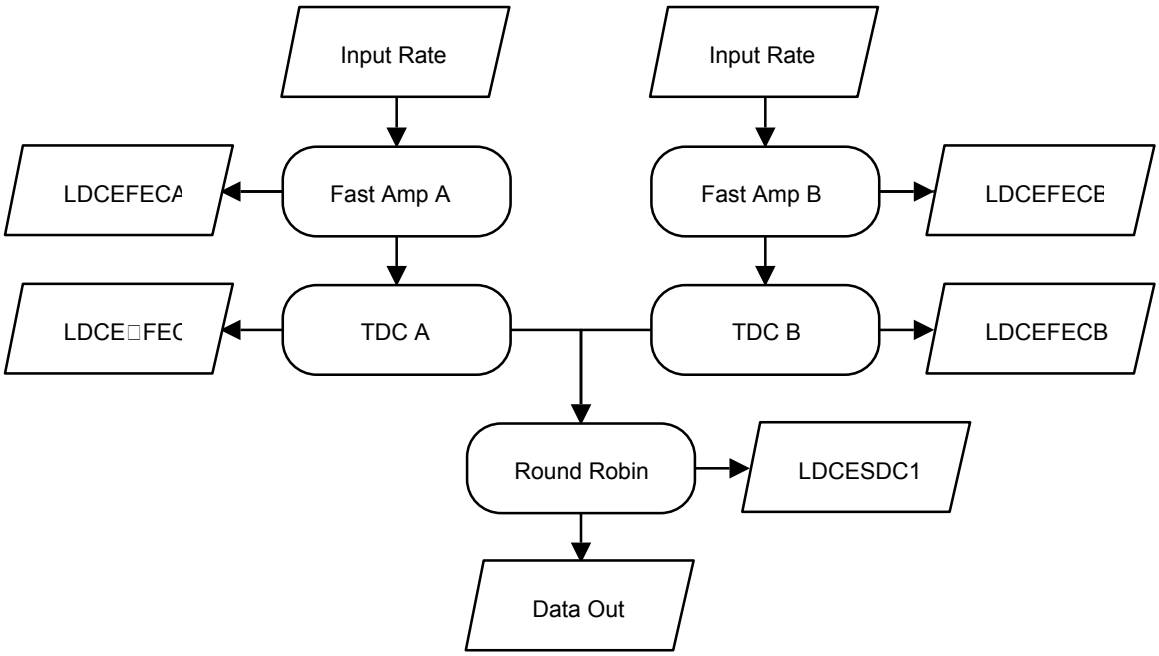

Figure 4.6-1: Flowchart representation of the counters in the FUV detector that are used to calculate the live time.

4.6.2 FUV Time Tag Data

As discussed above, the live time of an individual segment operating in TTAG mode may be computed through a variety of ways. They include the following:

1) Compute the time varying count rate and use ground calibration data to create a time varying live time correction.
2) Compute the average live time using the electronic stim data.
3) Compute the average live time correction from the engineering data (ED) snapshots present at the beginning and end of an exposure.

The first technique is the most accurate for TTAG data and shall be used to correct the data. The second two methods shall be used to verify the first method and shall also be used to determine the live time corrections for ACCUM data as discussed below.

The live time for TTAG data shall be determined by computing the output count rate of the detector segment for 10 seconds of data (see equation 4.6-2). Using this count rate the live time correction shall be determined from the ground calibration data and applied to those photons, which fall within the 10 second interval.

$$R_{seg}(t) = \frac{\sum_{t=t_0}^{t=t_0+10} \nu_t}{10.00} \qquad \text{Eqn. 4.6-2}$$

where

$R_{seg}(t)$ is the count rate for a 10 second interval starting at t0.
ν denotes a single event.
t is the arrival time of event ν.

The 10 second integration time is required to collect at least 100 counts. A dim target ($\sim 10^{-15}$ ergs/cm^2/sec/Å) for the FUV channel will have a minimum count rate of ~ 20 counts/second. In a 10 second integration 200 counts will be collected. For the NUV channel the background dominates signal at the 10^{-15} ergs/cm^2/sec/Å with about 250 counts/second, so achieving 100 counts is guaranteed in 10 seconds.

The live time is a function of the time varying count rate of the detector. In practical terms, the live time calibration shall be a lookup table with a live time versus measured count rate. In instances where the measured count rate falls between calibration points, linear interpolation shall be used at a minimum to determine the appropriate live time correction to apply to the data. More accurate methods for interpolating the live time correction data shall be acceptable.

The value of the live time shall be verified using electronic stim pin data. This is the second most accurate method for computing the live time of the detector. This value should closely match the value of the live time as determined from the ground calibration data. In this case the live time is computed using equation 4.6-3:

$$livetime_{seg} = \frac{C_{e-stims}}{R_{e-stims} * t_{exposure}} \qquad \text{Eqn 4.6-3}$$

where

$R_{e\text{-}stims}$ is the input rate of electronic stims.
$C_{e\text{-}stims}$ is the output number of e-stim events present in the exposure
$t_{exposure}$ is the exposure time.

seg is the segment identification.

The individual segment live time correction shall also be determined using the instantaneous digital event counter (LDCEDECA and LDCEDECB) values in the ED snapshots present at the beginning and end of a given exposure. These two values shall be averaged and used with the ground calibration data to determine the live time correction for that exposure.

The live times for each segment are scaled by the live time associated with the round robin following the example shown in equation 4.6-1 to derive the total live time for each segment.

4.6.3 FUV ACCUM Data

The live time correction for FUV ACCUM data shall be determined using the electronic stims as discussed in section 4.6.2

The value of the live time shall be verified using the instantaneous LDCEDECA and LDCEDECB values in the ED snapshots present at the beginning and end of a given exposure. These two values shall be averaged and used with the ground calibration data to determine the live time correction for that exposure.

4.6.4 NUV Time Tag Data

The NUV TTAG data shall be handled in the same manner as for the FUV TTAG data with one exception. The NUV detector does not support electronic stims, so it is not possible to compute the average live time.

For the NUV detector the output rate is monitored by LMEVENTS. Using this telemetry item and the live time calibration curve one can determine the instantaneous live time for the NUV detector.

4.6.5 NUV ACCUM Data

The live time correction for NUV ACCUM data shall be determined using the instantaneous count rate monitor values (LMEVENTS) in the ED snapshots present at the beginning and end of a given exposure. These two values shall be averaged and used with the ground calibration data to determine the live time correction for that exposure

4.7 DERIVATION AND ASSOCIATION OF ε FACTORS

ε is an inefficiency factor that represents the probability of a photon creating a detected event, thus for a single event the ε is an effective count. The ε shall be formed by multiplying the individual pixel relative quantum efficiency by the appropriate live time correction (section 4.6). It is assumed that ε varies only with position on the detector and does not vary with wavelength.

In the case of TTAG data an ε shall be assigned to each photon event based on the dispersion and cross dispersion location of the event in geometrically correct space. The ε for a photon event shall be computed by taking the inverse of the multiplication of the flat field by the time varying live time correction as shown in equation 4.7-1.

$$\varepsilon_{i,j}(t) = \frac{1}{ff(i,j) \cdot livetime(t)} \qquad \text{Eqn. 4.7-1}$$

where

$\varepsilon_{i,j}$ is the inefficiency factor for pixel i,j at time t.
ff(i,j) is the flat field response at pixel i,j and is essentially a P-flat (see section 3.4).
live time(t) is the live time for the data at time t.

For ACCUM data the ε data shall be maintained in an image array. The ε image array is simply the inverse of the product of the intermediate flat field (iFF) array (see Equation 4.5-1) and the constant average live time, only an average live time is appropriate for an ACCUM exposure, as discussed in section 4.6. Please see section 4.5.2 for a definition of an intermediate flat field.

4.8 ASSOCIATION OF DATA QUALITY FLAGS

Data quality flags, referred to as q, are numerical values which indicate whether the data associated with either a photon event, a pixel in an ACCUM image, or spectral resolution element is compromised by a known detector feature. For an individual photon event the data quality flag shall be read from a table that indicates the type of detector feature, the region where the feature could affect the data quality, and a numerical value for the feature. A list of potential features and their numerical values is shown in Table 3.5.

For an ACCUM image the observer will need to refer to the data quality reference table discussed in section 3.5. This table shall list the type of detector feature, the region where the feature could affect the data quality, and the numerical value for the appropriate type of feature.

For one-dimensional, extracted spectroscopic data the data quality flags are used to compute average and maximum data quality values for each resolution element. This is discussed further in section 4.13.

4.9 APPLYING DOPPLER CORRECTIONS

After the data are corrected for instrument induced distortions they shall be corrected for Doppler shifts due to orbital and heliocentric motion. Using orbital reference and target ephemeris data the orbital and heliocentric Doppler shifts shall be computed.

4.9.1 Orbital Doppler Correction

The orbital Doppler shift in units of pixels is computed via equation 4.9-1.

$$\Delta P_{orb}(\lambda,t) = C(\lambda,t)\sin\left\{\left[2\pi(t-t0)\right]/P\right\} \qquad \text{Eqn. 4.9-1}$$

where

C(λ,t) is the maximum Doppler shift for the target (see equation 4.9-2).
t is the current time during an exposure.
t0 is the time the HST passed the target's orbital longitude (time of zero Doppler shift).
P is the HST orbital period.

$$C(\lambda,t) = \frac{\lambda}{c \cdot p} V_{HST} \cdot \left|\hat{n}(t) \times \hat{T}\right| \qquad \text{Eqn. 4.9-2}$$

where

λ is the wavelength of light.
c is the speed of light.
p is the average plate scale in Å/pixels (see Table 4.9-1 for the plate scale for each spectroscopic mode).
V_{HST} is the orbital velocity of the Hubble Space Telescope.
$\hat{n}(t)$ is the unit vector normal to the HST orbital plane and is defined by equation 4.9-3 in a geocentric coordinate system.
$\hat{t}$ is the unit vector towards the target in a geocentric coordinate system.

$$\hat{n}(t) = \left[\sin(i)\sin(\theta(t)), -\sin(i)\cos(\theta(t)), \cos(i)\right] \qquad \text{Eqn. 4.9-3}$$

where

i is the inclination of the HST orbital plane.
θ is the longitude of the HST ascending node, eastward from RA=0.

Table 4.9-1

Plate Scales for COS Spectroscopic Modes*	
G130M	~0.0094 Å/pixel
G160M	~0.0118 Å/pixel
G140L	~0.0865 Å/pixel
G185M	~0.0273 Å/pixel
G225M	~0.0342 Å/pixel
G285M	~0.0400 Å/pixel
G230L	~0.3887 Å/pixel

* These values are derived from raytrace models. Final values will need to be inserted after instrument calibration is complete.

4.9.2 Heliocentric Doppler Correction

Heliocentric Doppler corrections are made via equation 4.9-4.

$$\Delta P_{helio}(\lambda,t) = \frac{-\lambda_{obs}}{p}\left(\frac{\vec{v}(t)\cdot\hat{T}(t)}{c}\right) \qquad \text{Eqn. 4.9-4}$$

where

ΔP_{helio} is the heliocentric Doppler shift in pixels
p is the dispersion in Å/pixel (see Table 4.10-1)
λ_{obs} is the observed wavelength in Å.
v = 29.786 km/sec and is the Earth's velocity relative to the Sun in equatorial coordinates.
c = 299792.458 km/sec is the speed of light.
$\hat{T}$ is the unit vector towards the target in equatorial coordinates.

The components of $\dot{v}$ are shown in equations 4.9-5 through 4.9-7

$$v_0 = -|\vec{v}|\sin(Le) \qquad \text{Eqn. 4.9-5}$$
$$v_1 = |\dot{v}|\cos(Le)\cos(eps) \qquad \text{Eqn. 4.9-6}$$
$$v_2 = |\dot{v}|\sin(eps)\cos(Le) \qquad \text{Eqn. 4.9-7}$$

where

Le = 100.461 + 0.9856474 * (mjd – 51544.5) degrees and is the ecliptic longitude of the Earth.
mjd is the Modified Julian Date at the middle of the exposure.
eps = 23.439 degrees

4.9.3 TTAG MODE

For FUV and NUV TTAG data the wavelength dependent Doppler corrections shall be done as follows:

1) Compute the photon's approximate wavelength using the standard wavelength solution (see equation 4.9-1).
2) Compute the expected Doppler shift for the arrival time and wavelength of the photon using the approximate wavelength via equations 4.9-1 and 4.9-4.
3) Subtract $\Delta P_{orb}(\lambda, t)$ and $\Delta P_{helio}(\lambda, t)$ from P_x, the dispersion location of the photon (see equation 4.9-5)

$$P_x^{'} = P_x - \Delta P_{orb}(\lambda, t) - \Delta P_{helio}(\lambda, t) \qquad \text{Eqn. 4.9-5}$$

where

P'_x is the new pixel number for the Doppler corrected data.
P_x is the pixel number to be corrected.
ΔP_{orb} is the orbital Doppler correction in pixels.
ΔP_{helio} is the heliocentric Doppler correction in pixels.

The error introduced by applying the baseline wavelength solution to the data is insignificant. At 1000Å, a 1Å error in the initial wavelength identification introduces a ~130 μÅ error in the Doppler correction, 2 orders of magnitude below the specification for wavelength knowledge (this includes maximum heliocentric and orbital Doppler shifts).

4.9.4 ACCUM MODE

In ACCUM mode, onboard software partially corrects for orbital Doppler shifts induced by the orbit of HST around the Earth. The onboard Doppler compensation only corrects for Doppler effects *after* the beginning of the exposure, so there is a residual Doppler shift associated with where in the orbit the exposure began, i.e. the beginning of the

exposure does not correspond t0=0. Therefore, a one-time adjustment to the data for orbital and heliocentric Doppler shifts is required.

The offset for wavelength shifts due to orbital motion is given by equation 4.9-1, where t is replaced with t_{exp}, the time for the beginning of the exposure. The wavelength of each pixel shall be computed via equation 4.10-1. Corrections for the Doppler offsets $\Delta P_x(\lambda,t)$ shall be made to the data after the spectrum is extracted from the data to minimize degradation of the data due to resampling.

The large band-passes covered by the FUV spectra and multiple spectra associated with the NUV channel raise the possibility of differential Doppler shifts across the spectrum, in the FUV case, and between the spectral stripes in the NUV case. Calculations demonstrate that there is <1 FUV pixel and <0.2 NUV pixels of differential Doppler shifts, or equivalently <2 km/s error in the wavelength identification. The specification for absolute wavelength knowledge is <15 km/s, so correcting for this differential Doppler shift is not required. In summary, all Doppler shifts associated with orbital or heliocentric shifts shall be treated uniformly with no relative variation with wavelength. Finally, the differential shifts are small enough that blurring of the spectra will be minimal and resolution will be maintained.

Table 4.9-2

Calibration Constants		
Speed of light	**c**	2.99792458 x 10^5 km/sec
Orbital velocity of the Earth about the Sun	**v**	29.786 km/sec
Orbital velocity of HST	$\mathbf{v_{HST}}$	7.553577137408 x 10^3 m/sec
Plates scales for each spectroscopic mode		See Table 4.9-1

4.10 WAVELENGTH CALIBRATION

The instrumental wavelength scale for each of the COS operational modes shall be a low order polynomial function of the form shown in equation 4.10-1. The wavelength calibration spectra shall also require unique wavelength calibrations. Note that the wavelength scale is applied to the Doppler corrected dispersion coordinate (referred to as xd in section 2).

$$\lambda(P_x) = a_0 + a_1 P_x + a_2 P_x^2 + a_3 P_x^3 \qquad \text{Eqn. 4.10-1}$$

where

P_x is the Doppler corrected pixel value in the dispersion axis
$a_{0\text{-}3}$ are coefficients contained in the appropriate reference file
λ is the wavelength in Å

Prior to applying the final wavelength calibration the data shall be corrected for instrument induced shifts due to mechanism hysteresis and thermally induced distortions of the optical bench. These shifts can be tracked using the wavelength calibration spectra. To do this the following steps shall be taken…

1) Compare two in-flight wavelength calibration spectra and the wavelength calibration reference spectrum. In this case all spectra are in counts per pixel. Determine the offsets in the dispersion direction between these spectra using a cross-correlation technique and compute an average offset in pixels (ΔP).
2) Adjust each of the photon events by the calculated offset. This effectively brings each photon onto the correct wavelength scale (see equation 4.10-2).

$$P_x^{'} = P_x - \Delta P \qquad \text{Eqn. 4.10-2}$$

where

P'_x is the new pixel number on the correct wavelength scale.
P_x is the pixel number to be adjusted.
ΔP is the wavelength correction in pixels.

The basic assumption in this flow is that the offsets only affect the a_0 term in the wavelength scales. This assumption is sound because shifts will be due to repositioning of the spectra on the detector and not changes in the dispersion relation, i.e. the higher order terms in the wavelength solution.

For ACCUM data the wavelength offset ΔP shall be applied to the final wavelength scale.

Table 4.10-1

Calibration Constants		
Zero order polynomial term	a_0	TBD
First order polynomial term	a_1	TBD
Second order polynomial term	a_2	TBD
Third order polynomial term	a_3	TBD

4.11 FILTERING OF DATA BASED ON PULSE HEIGHT & TIME

4.11.1 Time Tag Data

A 5-bit pulse height value is associated with each detected TTAG event. The value of this pulse height is an indication of the validity of the detected event and can be used to exclude events that may not be real photon events. The event is excluded by comparing the value of the pulse height against upper and lower threshold values. Events that are below the lower level threshold or above the upper level threshold shall be culled from the data. The values of the upper and lower thresholds shall be maintained in a reference file (see section 3.8).

4.11.2 ACCUM Data

ACCUM data do not provide pulse height information for individual photons, so it is not possible to threshold data in the same way as is done for TTAG exposures. Accompanying each ACCUM image is a pulse height distribution (PHD), which is a histogram of the pulse heights for all of the detected events. Comparing the average and peak of the PHD can be used to confirm the detector was operating correctly and that no events occurred during the observation that might compromise the data. For example, in a typical PHD the peak and mean of the distribution are within 10% of each other. However, if the detector had an unusually high background the average will be significantly lower than the peak (see Figure 4.11-1). Furthermore, the peak should always be above a minimum value for the gain.

Therefore, for an ACCUM exposure the peak and average of the PHD shall be computed. The exposure shall be deemed acceptable if the average is within 20% of the peak channel. Furthermore, the peak shall be above a minimum value and below the upper level threshold.

4.11.3 Isolation of Specific Observation Times

The capability shall also be implemented that TTAG data, which were acquired during specific periods of time, can be excluded from the analysis. In general this capability will be used if known events that could impact the quality of the data, e.g. a solar storm, can be excluded from the data.

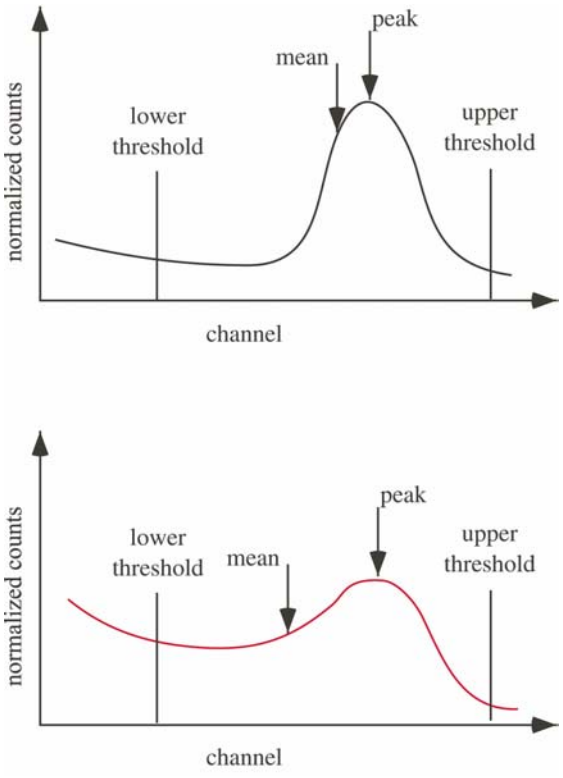

Figure 4.11-1: The upper panel shows "good" pulse height distribution for an observation. The lower panel shows what the pulse height distribution might look like with an anomalous background. Notice how the peak and mean vary depending upon the shape of the distribution. The lower threshold (LLT) will be determined from gain maps taken during ground calibration and eventually from flight data.

Table 4.11-1

Calibration Constants		
Lower level threshold	**LLT**	See OP-01 for details
Pulse Height Distribution	**PHD**	"
Upper level threshold	**ULT**	"
Mean of Pulse Height Distribution	**MPHD**	TBD
Peak of Pulse Height Distribution	**PPHD**	TBD

4.12 CREATION OF 2-D IMAGE PRODUCTS

This is the final step in processing the raw science data in preparation for creating the flux-calibrated spectrum. For correct error propagation and analysis, two images shall be produced, one with raw counts/second and another with effective counts/second. The effective counts/second image is a final data product delivered to the observer. The counts/second image is an intermediate data product that is only necessary for subtracting the intrinsic detector background and for computing the statistical errors and shall not be delivered to the observer.

4.12.1 TTAG Data

The 2-D count image shall be created by incrementing the value of the pixel for each photon where P_i-1/2 < P_x < P_i +1/2 and P_j-1/2 < P_y < P_j +1/2. The image shall be 16384 X 1024 pixels for the FUV data and 1024 X 1024 for the NUV data. This image is referred to as the C image (see equation 4.12-1).

$$C_{jk} = \sum_i \delta_{ijk} \quad \text{where } \delta_{ijk} = 1 \text{ if } P_j\text{-}1/2 < P_x < P_j + 1/2 \quad P_k\text{-}1/2 < P_y < P_k + 1/2 \qquad \text{Eqn. 4.12-1}$$

The 2-D effective count image shall be identical in size to the 2-D count image. However, the value at each pixel location shall be the sum of the ε values for all the events associated with that pixel (see equation 4.12-2). This image is referred to as the E image.

$$E_{jk} = \sum_i \varepsilon_{ijk} \cdot \delta_{ijk} \quad \text{where } \delta_{ijk} = 1 \text{ if } P_j\text{-}1/2 < P_x < P_j + 1/2 \quad P_k\text{-}1/2 < P_y < P_k + 1/2 \qquad \text{Eqn. 4.12-2}$$

After each image is formed the actual (not commanded) exposure time shall be divided into the array so that the final product is in units of counts/second or effective counts/second.

4.12.2 ACCUM Data

For FUV ACCUM data the 2-D count and effective count images are computed in the same way as for TTAG data (see Figure 4.1-3).

The NUV ACCUM data is even simpler. The raw NUV detector image is the 2-D count image and the flat-fielded image is the 2-D effective count image (see Figure 4.1-6).

After both images are formed the exposure time shall be divide into each array so that the final product is in units of counts/second.

4.12.3 Generation of the Error Image

Per section 2 of this document an error array shall be provided to the observer as a data product. The error in each pixel shall be computer per equation 4.12-3. Equation 4.12-3 assumes that the detector does not alter the counting statistics in any way. While this is likely a valid assumption, it shall be verified during instrument level testing, when the full electronic chain will be in place.

$$\sigma_{E_{ij}} = \langle \varepsilon_{ij} \rangle \sqrt{C_{ij}} \qquad \text{Eqn. 4.12-3}$$

4.13 EXTRACTING RAW SCIENCE SPECTRA

Extracting the raw science spectrum shall include the following steps; extracting the science spectrum, extracting the background spectrum, associating data quality flags, and producing a background subtracted spectrum with associated data quality flags. Extracting the science spectrum shall produce a tabular data product consisting of 7 columns and 16384 rows for FUV data and 1024 rows for NUV data. The data in each column shall be wavelength, gross count rate (GC), background count rate (BK), net count rate (N), the error (σ), the maximum data quality (MDQ), and the average data quality (ADQ).

4.13.1 FUV Data

The wavelength for each bin is computed using equation 4.10-1 with the coefficients appropriate for the instrument configuration. In the case of the FUV data, all the events are on a common wavelength scale as discussed in section 4.10.

The center of the FUV spectrum in the spatial dimension for each detector segment shall be described by a linear function of the form shown in equation 4.13-1 and detailed in table 4.13-1.

$$P_y = m_{seg} P_x + b_{seg} \qquad \text{Eqn. 4.13-1}$$

The extraction limits about the function P_y are defined in Table 4.13-1 (also see Figure 4.13-1). Similarly, the background shall be described by a linear function with the same slope as equation 4.13-1, but with different b_{seg}.

The gross count rate (GC_i), background count rate (BK_i), and net count rate (N_i) for spectral element i are then computed from within the extraction limit. Equations 4.13-2 through 4.13-4 show how GC_i, BK_i, and N_i are computed.

$$GC_i = \sum_{j=m\cdot i+b1-\Delta n}^{m\cdot i+b1+\Delta n} C_{ij} \qquad \text{Eqn. 4.13-2}$$

$$BK_i = \frac{\Delta n}{\Delta w \Delta n2} \sum_{i=i-\Delta w}^{i=i+\Delta w} \frac{1}{2} \left\{ \sum_{j=m\cdot i+b2-\Delta n2}^{m\cdot i+b2+\Delta n2} C_{ij} + \sum_{j=m\cdot i+b3-\Delta n2}^{m\cdot i+b3+\Delta n2} C_{ij} \right\} \qquad \text{Eqn. 4.13-3}$$

where

C_{ij} is the counts in a single pixel in the count image (see section 4.12)
Δw is the width in the spectral direction over which the background is averaged.

The background BK_i is the local average of the background. The local average shall be computed using the background bins within $\pm \Delta w/2$ bins of the central bin (see equation 4.13-3). This averaging is done to minimize degradation of the final signal-to-noise from Poisson noise in the background, where the events are fewer. If there are areas of the background region that are know to be anomalous in some way, e.g. dead spots or strong hot spots, they may be excluded from estimate of the background.

The net count, N_i, is the flat field corrected count rate for the spectral bin i. The Doppler corrections made to the photons positions allows for photons within a given pixel or wavelength bin to have different ε_{ij} terms. Therefore, in computing N_i a weighted average shall be employed. The following is a brief derivation of N_i that is included for clarity.

Consider a spectral bin i as shown in figure 4.13-2. Spectral bin i is composed of multiple pixels in the cross dispersion direction. The effective counts in a pixel is the sum of all the ε_{ij} within that pixel and is NOT the number of events multiplied by the ε_{ij} for that pixel (as would be the case for a charge-coupled device). Therefore, an average ε_{ij} must be employed at the pixel and spectral bin levels (see equations 4.13-4 and 4.13-5). N_i is then the gross count rate minus the background count rate and multiplied by the average ε_i for that spectral bin (see equation 4.13-6). A further discussion and derivation of equation 4.13-6 is presented in section 7 of this document for clarity and historical purposes.

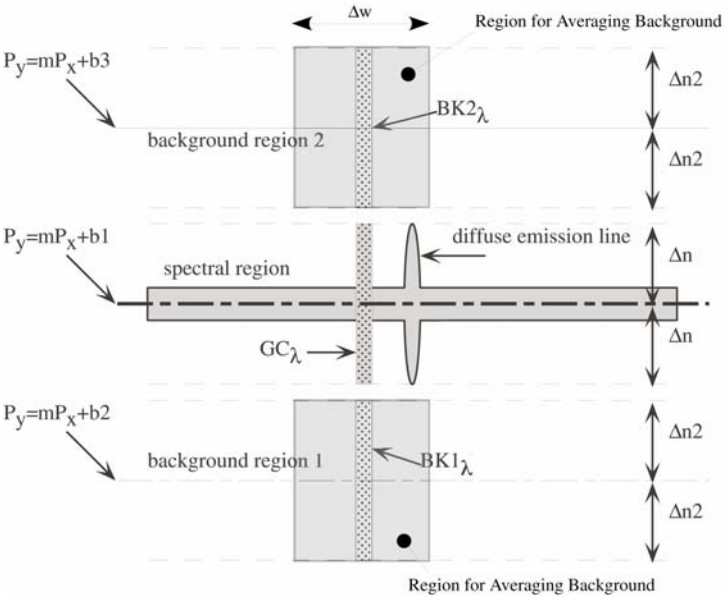

Figure 4.13-1: Spectral and background extraction regions.

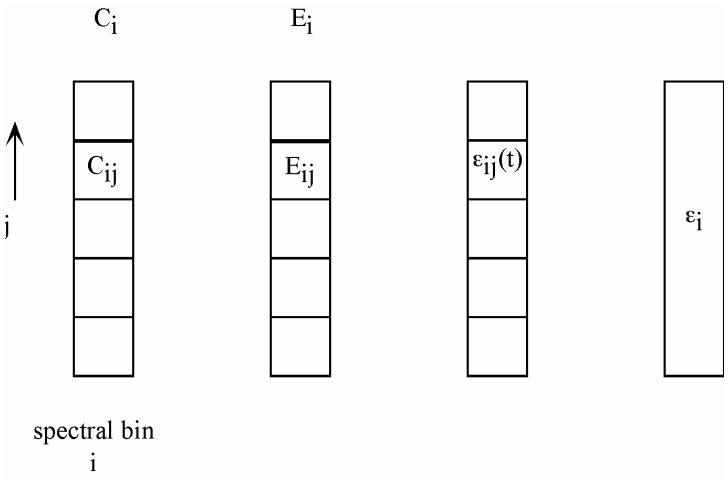

Figure 4.13-2: Schematic representation of equations 4.13-4 through 4.13-6.

$$\langle \varepsilon_{ij} \rangle = \frac{E_{ij}}{C_{ij}} \qquad \text{Eqn. 4.13-4}$$

$$\varepsilon_i = \frac{\sum_j \varepsilon_{ij} C_{ij}}{\sum_j C_{ij}} = \frac{\sum_j \frac{E_{ij}}{C_{ij}} C_{ij}}{\sum_j C_{ij}} = \frac{\sum_j E_{ij}}{\sum_j C_{ij}} = \frac{E_i}{C_i} \qquad \text{Eqn. 4.13-5}$$

$$N_i = \varepsilon_i (GC_i - BK_i) = \frac{E_i}{C_i} (GC_i - BK_i) \qquad \text{Eqn. 4.13-6}$$

The final form of the error for the raw spectrum (equation 4.13-6) in counts per second is then given by equation 4.13-7. The derivation is presented in section 7 of this document.

$$\sigma_{N_i} = \frac{1}{t_{\exp}} \sqrt{\left(N_i t_{\exp} \frac{1}{N_j \cdot SNR_{ff_{ij}}} \right)^2 + \varepsilon_i^2 t_{\exp} \left(GC_i + \left(\frac{\Delta n}{\Delta w \Delta n_2} \right) BK_i \right)} \qquad \text{Eqn. 4.13-7}$$

where

N_j is the number of rows combined into a spectral bin.
SNR_{ffij} is the signal-to-noise ratio of the flat field data at the pixel level.
t_{exp} is the exposure time.

For a spectral resolution element (N_i) the average (ADQ_i) and maximum (MDQ_i) data quality are computed based on the individual values associated with the photon events or location in the ACCUM image. These two values will indicate to the observer whether a spectral resolution element falls near a blemish (MDQ) and then how badly the data are compromised (ADQ). The ADQ shall be computed using equation 4.13-8

$$adq_i = \frac{1}{n} \sum_{j=m \cdot i + b1 - \Delta n}^{m \cdot i + b1 + \Delta n} n_{ij} q_{ij} \qquad \text{Eqn. 4.13-8}$$

where

i denotes a spectral bin.
n_{ij} is the number of counts in pixel i,j.
n is the total number of counts within the region (=sum(n_{ij}))
q_{ij} is the quality factor associated with that pixel and from the lookup table discussed in section 4.8.

Table 4.13-1

Calibration Constants		
Slope,	**m**	TBD
y-intercepts		
Spectrum	$\mathbf{b_{seg}}$	TBD
Background region 1	$\mathbf{b_{bk1}}$	TBD
Background region 2	$\mathbf{b_{bk2}}$	TBD
Spectrum extraction half height	**Δn**	TBD
Background extraction half height	**Δn2**	TBD
Background extraction width	**Δw**	TBD

4.13.2 NUV Data

For the NUV data the methodology for extracting a raw spectrum is identical to how raw FUV spectra are extracted with a couple of exceptions. The wavelength for each bin is computed using equation 4.10-1 with the coefficients appropriate for the instrument configuration and spectral stripe. The NUV spectra, however, are NOT on a common wavelength scale unlike the FUV spectra as mentioned at the very end of section 4.10. This affects how the individual spectra are co-added and is discussed further in section 4.16.

Each spectral stripe shall be described by a linear function of the form shown in equation 4.13-1 and using the spectral extraction regions shown in figure 4.13-3 and detailed in Table 4.13-2.

The NUV channel design suffers from a problem unique to diffuse targets that fill the entrance aperture. Figure 4.13-4 shows the raytrace spots for three monochromatic wavelengths from the NCM3a, NCM3b, and NCM3c camera optics. In each case the aperture is fully illuminated. Notice that the three images *overlap* over about 1/5 of their area. This overlap makes it very difficult to achieve any precision in the photometric calibration of the NUV channel in the case where the object is diffuse.

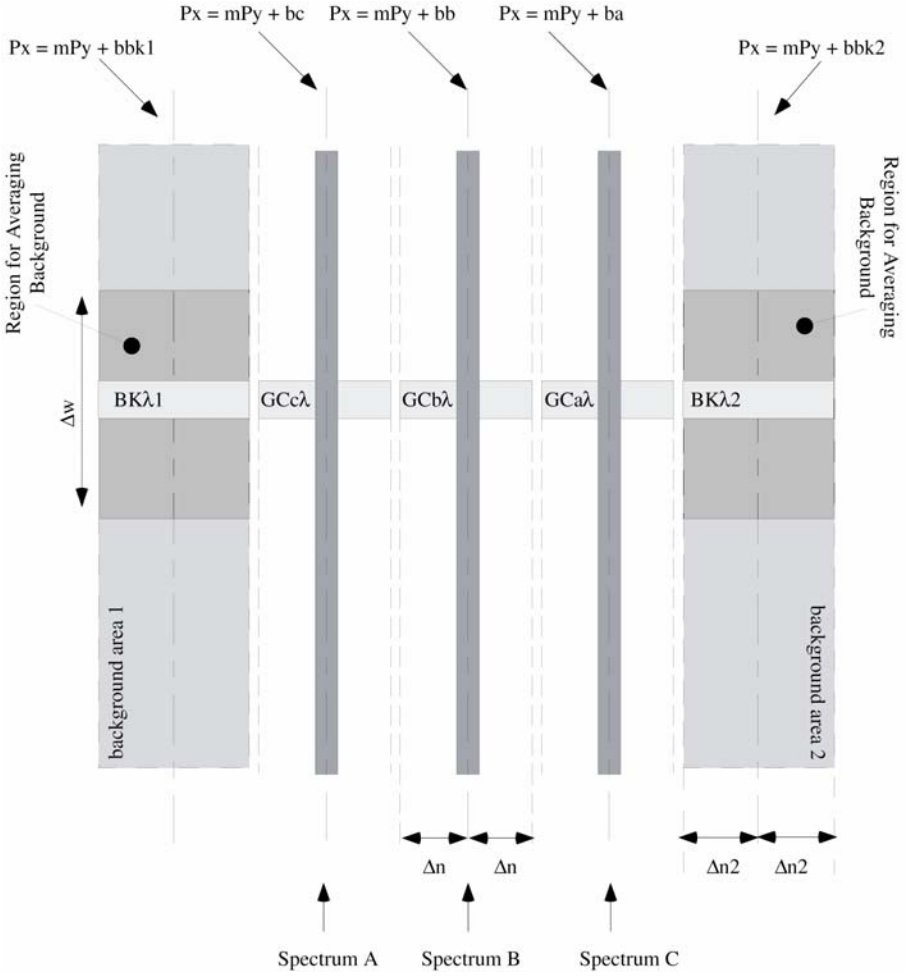

Figure 4.13-3: NUV spectral and background extraction regions.

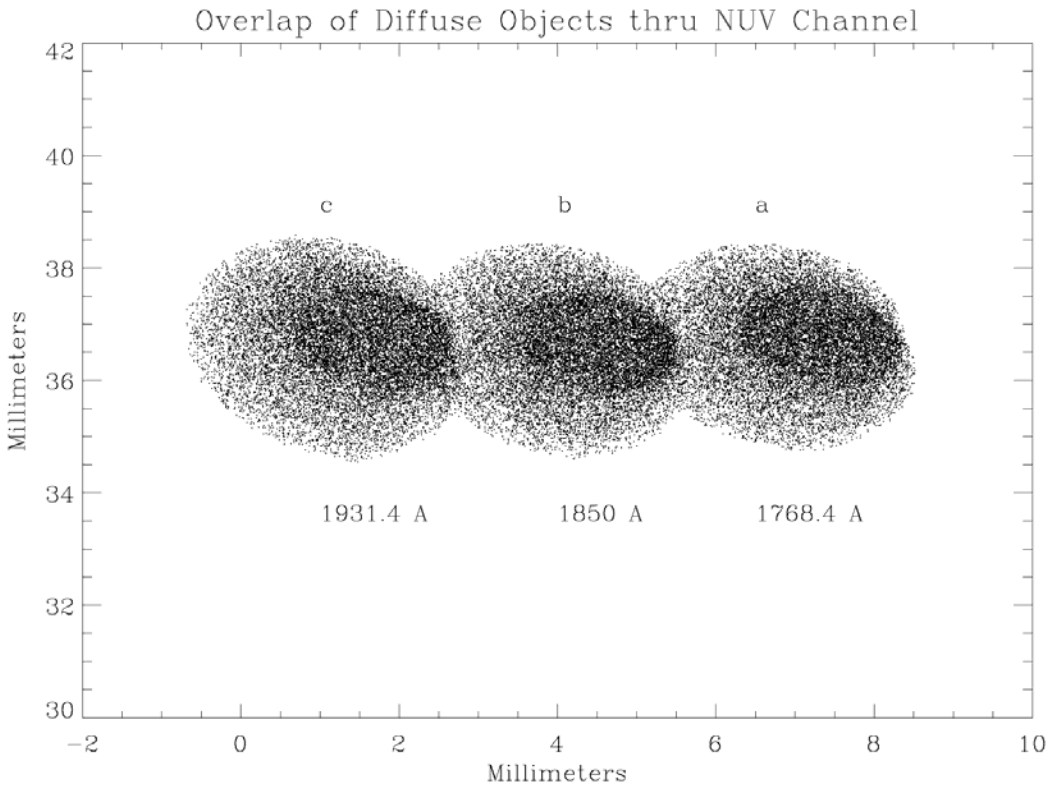

Figure 4.13-4: Raytrace models demonstrating how the NUV spectra can overlap in the case of a diffuse object.

The IDT is aware of this issue and feels that a lack of photometric accuracy in the case of diffuse targets is acceptable. Therefore, in the case of diffuse targets the extraction regions for the NUV data shall be identical as for point source targets. The observer shall be warned of the problems associated with the photometric accuracy of the data, and can re-extract 1-d spectra using tailored extraction regions from the corrected 2-D image if they wish.

Table 4.13-2

Calibration Constants		
Slope	**m**	TBD
y-intercepts		
Spectrum A	$\mathbf{b_a}$	TBD
Spectrum B	$\mathbf{b_b}$	TBD
Spectrum C	$\mathbf{b_c}$	TBD
Background region 1	$\mathbf{b_{bk1}}$	TBD
Background region 2	$\mathbf{b_{bk2}}$	TBD
Spectrum extraction half height	**Δn**	TBD
Background extraction half height	**Δn2**	TBD
Background extraction width	**Δw**	TBD

4.14 CORRECTING FOR OTA & INPLANE GRATING SCATTER

Correcting for optical telescope assembly (OTA) and in-plane grating scatter depends on the specific spectrum observed by the instrument. Therefore, it is impossible for the reduction pipeline to correct for the scatter. Once the spectrum has been observed it is possible to correct for the scatter contributions and this shall be left to the observer.

The IDT shall endeavor to develop the appropriate algorithm for removing the contributions to the spectrum from scatter and make these algorithms available to the observing community. However, at this time there is insufficient understanding of the OTA scatter to provide meaningful guidance on this topic.

4.15 SENSITIVITY CALIBRATION

Conversion of the net count rate spectrum (N_i) to absolute flux is accomplished via equation 4.15-1.

$$F_\lambda = \frac{hcN_\lambda}{A_{HST}\lambda dT_\lambda^{sys}} \qquad (\text{ergs/cm}^2\text{/sec/Å}) \qquad \text{Eqn. 4.15-1}$$

where

F_λ is the calibrated flux at a specific wavelength.
h is Planck's constant (6.6256×10^{-27} ergs sec).
c is the speed of light ($2.99792458 \times 10^{10}$ cm/sec)
N_λ is the net count rate at a particular wavelength.

$A_{HST} = (\pi * 120^2) = 45238.93416$ cm^2 and is the geometric collecting area of the HST primary mirror.
T_λ^{sys} is the integrated system throughput (including the OTA central observation) at a particular wavelength (see section 3.2).
λ is the specific wavelength (Å).
d is the dispersion for wavelength λ in units of Å/pixel (see Table 4.9-1 for approximate values for each spectroscopic channel).

Applying the flux calibration to the raw spectra shall produce a tabular data product consisting of 8 columns and 16384 rows for FUV data and 1024 rows for NUV data. The data in each column shall be wavelength (λ), flux (F) in units of ergs/cm^2/sec/Å, gross count rate (GC), background count rate (BK), net count rate (N), the maximum data quality (MDQ), average data quality (ADQ), and the error (σ) in units of ergs/cm^2/sec/Å.

Table 4.15-1

Calibration Constants		
Speed of light	**c**	2.99792458 x 10^{10} cm/sec
Geometric collecting area of HST	$\mathbf{A_{HST}}$	45238.93416 cm^2
Plate scales for each spectroscopic mode		See Table 4.9-1
Planks constant	**h**	6.6256 X 10^{-27} ergs sec

4.16 MERGING OF FP SPLIT DATA

The current plan is that each observation will be broken up into four separate exposures, each taken with the grating at a slightly different angle to help minimize the effects of detector fixed pattern noise in the final spectrum. To this end, the multiple flux-calibrated spectra from the sub-exposures shall be combined to form the final science spectrum.

For TTAG and ACCUM data the merged spectrum shall consist of a tabular data product consisting of 8 columns and 16384 rows for FUV data and 1024 rows for NUV data. The data in each column shall be wavelength (Å), flux (F) in units of ergs/cm^2/sec/Å, gross count rate (GC), background count rate (BK), net count rate (N), the error (σ) in units of ergs/cm^2/sec/Å, the maximum data quality (MDQ), and the average data quality (ADQ)..

There may remain in the spectra differences in the wavelength scales that might degrade the resolution if the spectra were simply co-added. Therefore, prior to co-adding the wavelength scales of each spectrum shall be adjusted slightly so that all the spectra will lie on the same wavelength scale. The wavelength offsets shall be determined using a

cross-correlation technique applied to the individual wavelength calibration spectra and then applied to the individual science spectra.

After the wavelength scales are adjusted they are then co-added as described by equation 4.16-1.

$$F_\lambda = \frac{\sum_i F_{\lambda i} \cdot t_i}{\sum_i t_i} \qquad \text{Eqn. 4.16-1}$$

where

F_λ is the flux at a specific wavelength.
λ is the specific wavelength.
n is the number of sub exposures per target.
t_i is the observation time
i denotes a specific wavelength bin

The error for the final merged spectrum is given by the expression in equation 4.16-2.

$$\sigma_{F\lambda} = \frac{1}{\sum_i t_i} \sqrt{\sum_i \left(t_i \sigma_{Fi}\right)^2} \qquad \text{Eqn. 4.16-2}$$

4.17 TA-1 IMAGE DATA

The TA-1 image data shall only be corrected for flat field variations as shown in figure 4.1-8.

TA-1 has a wide bandpass and no filter complement, so applying a flux calibration is meaningless without prior knowledge of the spectral distribution. Furthermore, the field of view of the TA-1 mode suffers from a radial vignetting function. While the calibration data from ground and in-flight testing shall exist, which will allow an observer to create their own flux calibrated image, there shall be no attempt made to routinely reduce TA-1 image data other than correcting for flat field variations.

5. GROUND CALIBRATION OF COS

5.1 INTRODUCTION

This section pertains to the calibration of the entire COS instrument prior to launch on SM-4. All reference files required to correctly reduce the initial flight data shall be produced using the ground calibration data. Subsequent observations of astrophysical targets shall be used to update the reference files for use by the reduction pipeline (see section 6 for details).

In this and the next section the terms "channel" or "mode" are synonymous and refer to the optical path selected within the COS instrument. For example, "G185M" is a mode or channel. A "configuration" of a "channel" or "mode" refers to a specific combination of aperture and central wavelength. As another illustration, there are 3 FUV modes and 16 FUV configurations (3 central wavelengths for the G130M and G160M gratings, 2 central wavelengths for the G140L grating, and either the primary science or bright object aperture).

5.2 STAFFING AND SUPPORT REQUIREMENTS

The facility where thermal vacuum testing and subsequent instrument calibration will occur has yet to be selected. However, it is possible to list the titles of the various team leaders and estimated staff to calibrate the instrument. They are as follows:

Title	Role
I&T Manager	Direct, plan, and schedule the calibration activity with inputs from the instrument and calibration scientists.
COS Instrument Scientist	Organize and verify that the required performance characteristics are calibrated.
COS Calibration Scientist	Verify the integrity of the calibration data and work with the instrument scientist to develop the plan for measuring the required performance characteristics.
Support Scientists (10)	Reduce the calibration data as it is acquired and extract the various calibration data.
Electrical Engineer/Technicians	Maintain the electrical systems for the instrument. Trouble shoot as required.
Mechanical Engineer/Technicians	Maintain the mechanical systems for the instrument. Trouble shoot as required.

	Only required during instrument installation and alignment in the vacuum chamber.
Facilities Engineer/Technicians	Maintain the test facilities. This is a full time position.

5.3 WAVELENGTH SCALE

Each channel and associated configuration shall have a unique wavelength scale of the form shown in equation 5.3-1. A table of offsets for each configuration shall be created that correct for offsets between the wavelength calibration spectra and the science spectra. These offsets are constant and due to differences in the illumination angle between the wavelength calibration optical path and the science optical path and the physical location of the wavelength calibration aperture with respect to the primary science aperture.

$$\lambda(P_x) = a_0 + a_1 P_x + a_2 P_x^2 + a_3 P_x^3 + \Delta a_{configuration} \qquad \text{Eqn. 5.3-1}$$

where

P_x is the Doppler corrected pixel value in the dispersion axis
$a_{0\text{-}3}$ are coefficients contained in the appropriate reference file
λ is the wavelength in Å
$\Delta a_{configuration}$ is the offset required to calculate the science spectrum wavelength scale. $\Delta\, a_{configuration} = 0$ for all wavelength calibration spectra and is non zero for science spectra.

The wavelength scale for each channel and configuration shall be determined as follows:

- Acquire a wavelength calibration spectrum in TTAG mode with a minimum of 1000 counts in at least 20 emission lines using the onboard wavelength calibration lamps.
- If the spectrum is an FUV spectrum then correct the detector image for thermal distortion (section 4.3) and geometric distortions (section 4.4).
- Create a 2-D image following the algorithm shown in section 4.12.1.
- Extract the image following the section 4.13.1 for the FUV or section 4.13.2 for the NUV channels.

- Fit gaussian line profiles to as many lines as possible and record the centroid for each gaussian profile. Each emission line shall have a minimum of 1000 counts total in the emission line.
- Using the Pt/Ne line list published in ApJ (Reader *et al* 1990, ApJ, **72**, 831.) identify the emission lines.
- Use a least squares routine fit a polynomial of the form shown in 5.3-1 to the centroid versus wavelength data.

The constant offsets between the wavelength calibration scale and the science wavelength calibration shall be determined as follows:

- Acquire a wavelength calibration spectrum in TTAG mode with a minimum of 1000 counts in at least 20 emission lines using the onboard wavelength calibration lamps.
- Acquire a spectrum of a Pt/Ne hollow-cathode lamp through the primary science aperture. In this case the Reflective Aberrated Simulator/Calibrator (RAS/Cal) shall be used to simulate the aberrated point spread function of the HST. The point spread function shall be centered in the primary science aperture to within 15 μm (0.05" in the HST focal plane).
- If the spectrum is an FUV spectrum then correct the detector image for thermal distortion (section 4.3) and geometric distortions (section 4.4).
- Create a 2-D image following the algorithm shown in section 4.12.1.
- Extract the image following the section 4.13.1 for the FUV or section 4.13.2 for the NUV channels.
- Apply the wavelength scale appropriate for that channel and configuration to both data sets.
- Fit gaussian line profiles to as many lines in each spectrum as possible and record the central wavelengths.
- Using a standard cross-correlation technique, compute the offset in angstroms required to line the science spectrum up with the calibration wavelength scale.
- Record this number for the channel being evaluated.

Ground testing of the FUV detector has shown that the geometric distortion depends upon high voltage of the detector (see CU document COS-11-0039). The geometric distortion cannot be directly measured in flight, however, it should be possible to correct the geometric distortion for variations due to changes in the high voltage using wavelength calibration spectra acquired at various high voltage levels. To that end, wavelength spectra shall be acquired in each configuration at±100 volt increments about the nominal high voltage. The number of increments, and thus range in high voltage, shall be sufficient to cover the expected operational range of high voltage, nominally the ±500 volts.

5.4 FOCUS CALIBRATION

Each optic on the OSM1 shall undergo a focus test. For the FUV channel a single central wavelength position of the grating is adequate. For the NUV channels the G185M and TA1 channels shall be used. The purpose of this calibration is to record the focus performance of the instrument versus position of the linear translation mechanism on OSM1. At discrete positions of the linear translation mechanism a wavelength calibration spectrum shall also be acquired.

The focus calibration shall be conducted as follows:

- The RAS/Cal system shall feed the COS instrument polychromatic light from a Pt/Ne hollow cathode lamp. The PSF shall be centered in the PSA to within 15 μm (0.05" in the HST focal plane).
- Acquire a spectrum of the RAS/Cal Pt/Ne lamp in TTAG mode. For the FUV channels there shall be a minimum of 1000 counts in at least 20 emission lines using the onboard wavelength calibration lamps. For the NUV channels there shall be a minimum of 3 lines per spectral stripe and 9 total with at least 1000 counts in each line.
- Immediately following the acquisition of the RAS/Cal spectrum acquire a wavelength calibration spectrum using the onboard wavelength calibration lamp.
- Reposition the linear stage and repeat until the full travel of the linear translation mechanism has been covered. The linear translation mechanism position shall be incremented in 0.5 mm steps, for a total of 28 science and 28 wavelength calibration exposures.
- Between the FUV and NUV channels the aperture mechanism may need to be repositioned depending upon the final optical alignments.

Each exposure shall be analyzed as follows:

- If the spectrum is an FUV spectrum then correct the detector image for thermal distortion (section 4.3) and geometric distortions (section 4.4).
- Create a 2-D image following the algorithm shown in section 4.12.1.
- Extract the image following the section 4.13.1 for the FUV or section 4.13.2 for the NUV channels.
- Fit gaussian line profiles to as many lines as possible and record the 1 σ width and centroid for each emission line. Each emission line shall have a minimum of 1000 counts total in the emission line. Also calculate the TBD % encircled energy of the line spread function for each emission line.
- Finally, plot the 1 σ width and encircled energy for each line versus the linear translation mechanism position.

5.5 SPECTRAL RESOLUTION

The spectral resolution of each channel and configuration shall be measured after the best focus is identified for each channel. The spectral resolution shall be measured using the RAS/Cal system with a Pt/Ne lamp. In addition, the spectral resolution of wavelength calibration spectra for each configuration shall also be measured. Spectral resolution is defined per the "Hubble Space Telescope Cosmic Origins Spectrograph Contract End Item (CEI) Specification" (STE-63) in section 4.3.2 "as the ratio $R=\lambda/\Delta\lambda$, where λ is the wavelength, and $\Delta\lambda$ is the measured Full Width at Half Maximum of a spectral feature whose intrinsic width is much narrower than the instrumental broadening." The spectral resolution for a single channel and configuration shall proceed as follows:

- The RAS/Cal system shall feed the COS instrument polychromatic light from a Pt/Ne hollow cathode lamp. The PSF shall be centered in the PSA to within 15 μm (0.05" in the HST focal plane).
- Acquire a spectrum of the RAS/Cal Pt/Ne lamp in TTAG mode. For the FUV channels there shall be a minimum of 1000 counts in at least 20 emission lines using the onboard wavelength calibration lamps. For the NUV channels there shall be a minimum of 3 lines per spectral stripe and 9 total with at least 1000 counts in each line.
- Immediately following the acquisition of the RAS/Cal spectrum acquire a wavelength calibration spectrum.
- If the spectrum is an FUV spectrum then correct the detector image for thermal distortion (section 4.3) and geometric distortions (section 4.4).
- Create a 2-D image following the algorithm shown in section 4.12.1.
- Extract the image following the section 4.13.1 for the FUV or section 4.13.2 for the NUV channels.
- Fit gaussian line profiles to as many lines as possible and record the 1 σ width and centroid for each emission line. Each emission line shall have a minimum of 1000 counts total in the emission line.
- Form the ratio $R= \lambda/\Delta\lambda$.

5.6 SPATIAL RESOLUTION

Per the "Hubble Space Telescope Cosmic Origins Spectrograph Contract End Item (CEI) Specification" (STE-63) section 4.3.3, "COS shall be capable of producing separate and distinguishable spectra for two point sources whose separation in the aperture is greater than 1.0 arc seconds." This specification applies to each channel as well. The spatial resolution of COS shall be verified at a minimum by characterizing the astigmatic height of the spectrum as a function of wavelength for each channel for a point source with a continuum spectrum. During ground testing it shall be adequate to use any suitable UV

light source and the RAS/Cal to create a suitable input function to COS for this test. By analysis the predicted separation required to produce separate and distinguishable spectra shall be computed.

If possible, RAS/Cal may be fitted with an aperture plate that has two point source apertures separated by 1 arc-second. Using any UV light source with the dual pinhole in RAS/Cal an image of the two point sources may be acquired. The image shall then be analyzed to determine if the two point sources are resolved.

5.7 SENSITIVITY CALIBRATION

Each channel and associated configuration shall be calibrated for efficiency. The efficiency shall be expressed as a number ranging from 0 to 1 in units of counts/photon, where the efficiency is the ratio of the output count rate to the input count rate. Therefore, efficiency equal to 0.5 means that 50% of the photons entering the instrument are detected.

For the FUV channels the efficiency shall be measured at a minimum of 12 uniformly distributed wavelengths across the operational bandpass of the channel. This includes the wavelengths covered by each configuration where the central wavelength is adjusted. Configurations associated with ±2 steps of the OSM1 to support FP Split observations are excluded from this requirement. Therefore, there shall be a total of 3 efficiency calibrations for the FUV configurations, each with 12 wavelengths measured for a total of 36 individual FUV exposures. In addition, the efficiency of the FUV channel shall be at 3 widely separated wavelengths in each configuration with the detector quantum efficiency enhancement grid OFF.

For the NUV channels the efficiency shall be measured at a minimum of 1 wavelength for each spectral stripe and for each central wavelength. Therefore, there shall be a total of 43 separate efficiency calibrations for the NUV channels. This is required because the incident angle changes significantly between different central wavelengths. This alters the groove efficiency profile of the grating and will ultimately change the efficiency curve.

The efficiency of both TA-1 modes, direct reflection and the front surface reflection off of the order sorter (“rear view mirror” mode), shall be measured in a similar fashion by introducing monochromatic point source images into the TA-1 channel and recording the measured count rate and the input count rate. The wavelengths shall cover the entire TA-1 bandpass. A minimum of 10 wavelengths shall be used. In addition, the sensitivity of the TA-1 mode shall be characterized as a function position within the aperture. The sensitivity as a function of position shall only be measured at the shortest and longest wavelengths.

Independent of the channel and configuration the efficiency for a single wavelength of light shall be measured as follows:

- Using the RAS/Cal, a monochromatic, aberrated beam of light shall be introduced into the center of the PSA. The PSF shall be centered in the PSA to within 15 μm (0.05" in the HST focal plane).
- Using the RAS/Cal measure the input rate to the aperture.
- Using COS acquire a TTAG data set with a minimum of 1000 events and 300 seconds of observing time.
- If the spectrum is an FUV spectrum then correct the detector image for thermal distortion (section 4.3) and geometric distortions (section 4.4).
- Calculate and assign the ε correction factors to each photon.
- Create a 2-D effective count image following the algorithm shown in section 4.12.1.
- Extract the spectrum following the section 4.13.1 for the FUV or section 4.13.2 for the NUV channels.
- Record the total number of events in the emission line.
- Divide the total number of effective counts by the exposure time to calculate the output count rate.
- Divide the output count rate by the input count rate to form the instrument efficiency for that wavelength.

5.8 FLAT FIELD RESPONSE

The flat field response shall be determined using the onboard flat field lamp and using a similar deuterium lamp passed through the RAS/Cal. This will allow the IDT to better understand the flat field performance derived from the onboard calibration lamps and from a stellar source. The results shall then be compared for consistency and any differences shall be studied and recorded to support the potential need for using stellar sources to derive flat fields in the event that onboard flat field calibration lamps fail.

The requirements for the flat field data are derived from a variety of documents that address the basic operational requirements of COS down to the practical implications of making flat field observations. Specifically, these are GSFC "Hubble Space Telescope Cosmic Origins Spectrograph Contract End Item (CEI) Specification" (STE-63), CU/CASA Technical Evaluation Report "FUV Detector Lifetime Estimates for Observation Planning" (COS-11-0018), and BASD Systems Engineering Reports "COS Signal to Noise Ratio and Flat Field Issues" (COS-Cal-001) and "Strategies for High Signal to Noise Ratio COS Spectra" (COS-Cal-008).

The primary requirement placed on the flat field data is that the signal to noise of the data shall be greater than or equal to 70:1 at the resolution element level. This assumes an observation that requires a signal to noise of 100 shall be comprised of four sub-exposures each with a signal to noise of 70:1 (COS-Cal-008). The large number of pixels provided by the detector makes it impractical and potentially detrimental to measure the flat field response at the pixel level due to concerns over the total exposure time (on order 50 hours) and the total charge extracted from the microchannel plate detectors (COS-11-0018).

The deuterium lamps onboard COS cover from 1150Å to 3200Å. At the shortest wavelength the deuterium lamp emits a dense forest of lines, which when blurred by the flat field aperture, forms a pseudo continuum. A 2Å resolution spectrum of a deuterium lamp is shown in figure 5.8-1 and is representative of what we can expect using the onboard flat field calibration system. This figure demonstrates that the flat field maps for each segment of the FUV detector will have to be created using different modes. Specifically, the flat field for segment A of the FUV detector shall be created using the G130M grating and that the flat field map for segment B shall be created using the G160M grating. The flat fields maps for the NUV grating shall be done using the G185M grating where the fluxes are fairly uniform with no strong features in the continuum. Figure 5.8-2 shows the spectral distributions across each segment of the FUV detector.

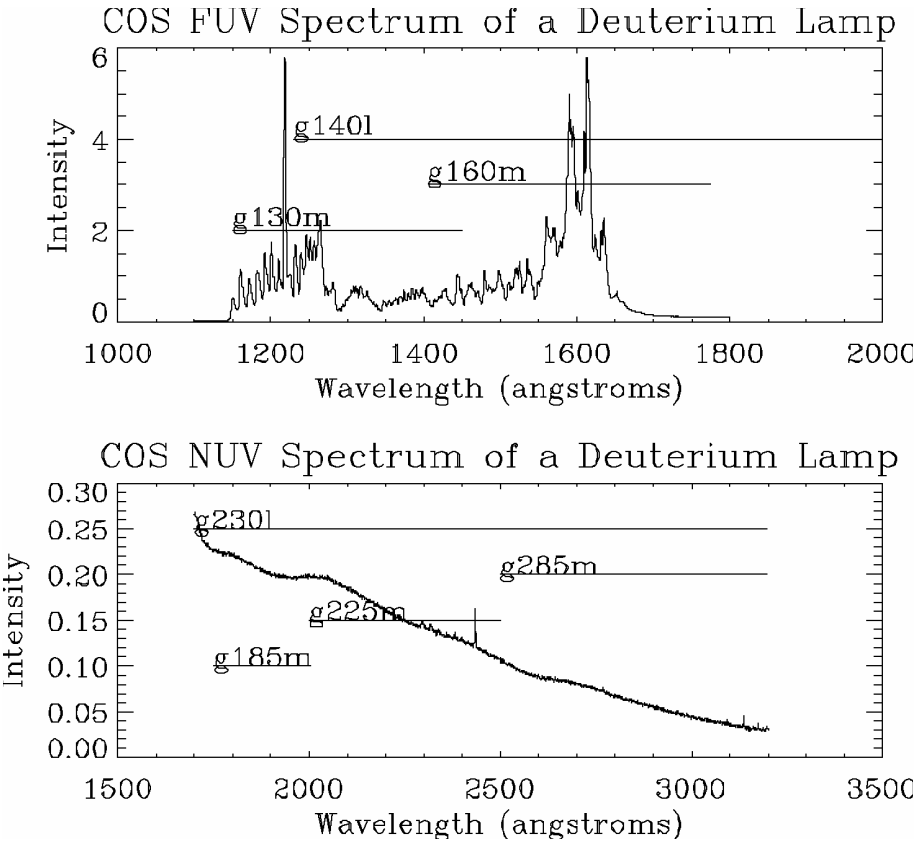

Figure 5.8-1: Measured spectrum of a deuterium lamp taken at 2Å resolution. The lamp is similar to the ones used in the COS flat field system.

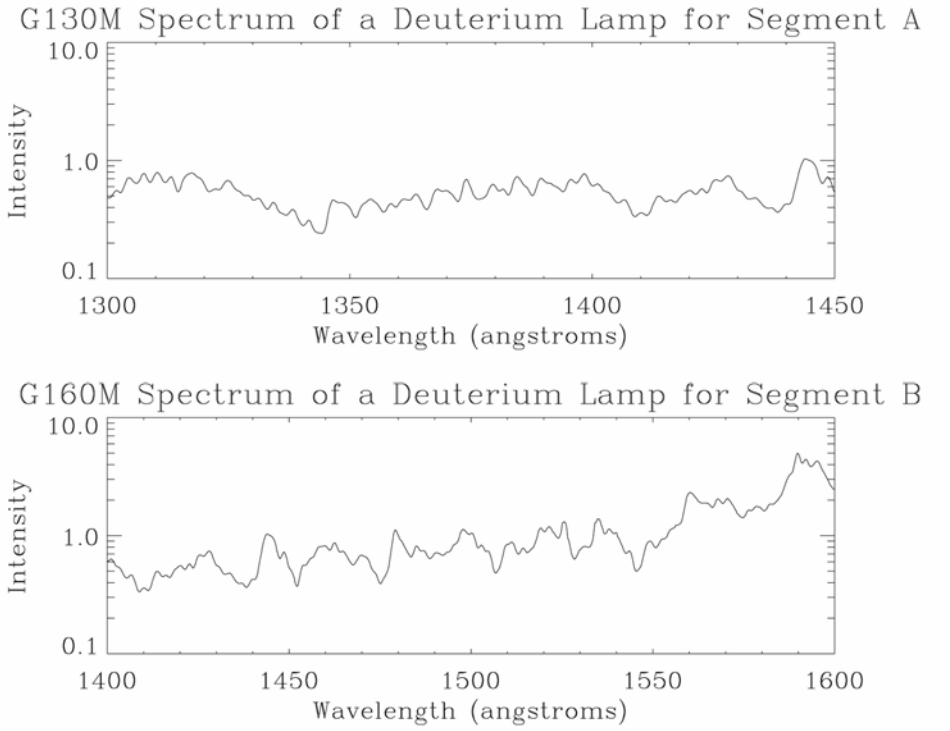

Figure 5.8-2: Expanded view of the deuterium spectrum for segment A using the G140L grating and segment B using the G160M spectrum.

Independent of the method used to introduce the light from deuterium lamp, either onboard system or RAS/Cal, or the channel the resolution element to resolution element response of the instrument shall be created as follows:

- Acquire a time tag data set with a minimum of 80 events per pixel or a minimum total number of events in the spectral region of 52,062,500. This will require about 2.5 hours of observation at 20,000 events/second.
- Correct the data back to the Baseline Reference Frame following the algorithm described in section 4.3.
- Correct the data for geometric distortions following the algorithm described in section 4.4.
- Resample the image into a 2-D array following the algorithm described in section 4.12.1.
- Create an L-fit by fitting a 2-D polynomial function of at least 10 degrees of freedom to the data. The L-fit shall replicate the low-frequency behavior of the spectrum to TBD%.

- Divide the L-fit into the raw 2-D image to create a P-flat. The P-flat will then contain values on order unity.

5.9 SIGNAL TO NOISE

Per the "Hubble Space Telescope Cosmic Origins Spectrograph Contract End Item (CEI) Specification" (STE-63) section 4.3.5, during instrument level calibration it shall be demonstrated that a signal to noise of 100:1 is possible. The signal to noise ratio of 100:1 shall be demonstrated at a minimum by using 4 sub-exposures that are then processed and co-added. Each sub-exposure shall be taken with the OSM1 mechanism in a slightly different configuration. At a minimum a signal to noise of 100:1 shall be demonstrated in a high resolution FUV mode and a high resolution NUV mode.

- Acquire in TTAG mode the 4 70:1 signal to noise spectra of a deuterium lamp through the RAS/Cal with an absorption cell in place (filled with an appropriate gas).
- Correct the data back to the Baseline Reference Frame following the algorithm described in section 4.3.
- Correct the data for geometric distortions following the algorithm described in section 4.4.
- Calculate and assign the ε correction factors to each photon per section 4.7.
- Resample the image into a 2-D array following the algorithm described in section 4.12.1.
- Extract the spectrum following the section 4.13.1 for the FUV or section 4.13.2 for the NUV channels.
- Bin the data into resolution element sized bins (approximately 6-7 high resolution bins).
- Co-add the spectra.
- Calculate the reciprocal of the root-mean-square (RMS) scatter of data points about a smooth function fit to those points away from the absorption line (N).
- The signal shall be calculated by subtracting off the flux as measured at the bottom of the absorption line from the continuum level (S).
- The signal to noise ratio is then the ratio of S/N.

5.10 CALIBRATION LAMP INTENSITY

There are four calibration lamps onboard the COS calibration delivery system, 2 Pt/Ne wavelength calibration lamps and 2 deuterium flat field lamps. The optical paths for each lamp are unique with slightly different efficiencies. In addition, each lamp can be operated at 3 current levels. Therefore, there are a total of 6 different intensity levels available for wavelength calibration and flat field calibration. Each of these intensity

levels shall be calibrated for future reference to monitor the degradation of the calibration subsystem performance due to contamination.

In addition, the intensity of the lamp versus time shall be measured for the minimum current level over a 10-minute period.

The configurations that shall be calibrated are presented in table 5.10-1.

Table 5.10-1

Lamp	Current Levels
Pt/Ne #1	**low**, medium, *high*
Pt/Ne #2	**low**, medium, *high*
D2 #1	**low**, medium, *high*
D2 #2	**low**, medium, *high*

bold text indicates the preferred current levels

italic text indicates current levels to avoid under normal circumstances or where the potential for permanently damaging the instrument exists. At these levels bright emission lines may exceed the maximum local count rates. Only test these levels if they are not expected to exceed the maximum local rates.

The calibrations shall proceed as follows:

- Configure COS to use the G160M channel.
- With the COS instrument on and ready to acquire data turn on a calibration lamp at the minimum current level and acquire a TTAG data set for 10 minutes.
- Then increase the lamp current to the intermediate setting and acquire a TTAG data set for 5 minutes.
- Finally, increase the current level to the maximum setting and acquire a TTAG data set for 5 minutes.
- Repeat this process for each lamp.
- Reconfigure COS into the G185M mode and repeat the lamp calibrations.

5.11 STRAY & SCATTERED LIGHT

Stray light is light incident on the detector active area that originates from a point or region within the COS instrument other than the diffractive surface of the grating in the optical path. Stray light can degrade the performance of the COS instrument and ultimately the quality of the data. In addition, stray light is very difficult to measure, as it often depends on the spectral distribution of the source being observed.

Scattered light is defined as polychromatic light incident on the detector active area that originates from the diffractive surface of the grating in the optical path. The scattered light shall be measured using an absorption cell and a deuterium continuum lamp.

Per the "Hubble Space Telescope Cosmic Origins Spectrograph Contract End Item (CEI) Specification" (STE-63) section 4.3.7 the stray and scattered light shall constitute less than "2% residual intensity to the signal in the core of a saturated absorption line measured with any of the high dispersion modes (GnnnM) in the spectrum of a point source in the PSA".

The stray and scattered light shall be measured as follows:

- Observe in TTAG mode the RAS/Cal and a deuterium lamp spectrum to create a spectrum with a minimum of 30:1 signal to noise per resolution element. An absorption cell shall be used to create a saturated absorption line in the continuum spectrum of the deuterium lamp.
- Correct the data back to the Baseline Reference Frame following the algorithm described in section 4.3.
- Correct the data for geometric distortions following the algorithm described in section 4.4.
- Calculate and assign the ε correction factors to each photon per section 4.7.
- Resample the image into a 2-D array following the algorithm described in section 4.12.1.
- Extract the spectrum following the section 4.13.1 for the FUV or section 4.13.2 for the NUV channels.
- Compare the continuum level to the level of the signal at the bottom of the absorption line.
- Using the fully corrected image examine the image for stray light.
- In addition, ex emission line spectrum can be used to measure the scattered and stray light. However, this is not the preferred method and shall be viewed as a secondary measurement.

5.12 STABILITY & REPEATABILITY

Per the "Hubble Space Telescope Cosmic Origins Spectrograph Contract End Item (CEI) Specification" (STE-63) section 4.3.8 changes in the position of the spectrum that occur on long time scales (>1 hr), referred to as drift, shall be less than 1 resolution element per hour. Furthermore, knowledge of the drift shall be provided that allows drift to be corrected to < 0.25 resolution elements. Changes in the position of the spectrum on short time scales (<1 hr), referred to as jitter, shall not "contribute more than 0.25 resolution

elements to the FWHM" of a resolution element.

Drift is due to changes in the position of any component in the optical path, thermal distortions in encoding the position of a photon, and many other unspecified effects. Jitter is due to random variations on short time scales and is dominated by high frequency pointing errors and vibration effects associated with the HST spacecraft. In ground testing drift shall be characterized during thermal vacuum testing as follows:

- During thermal vacuum testing of the instrument spectra shall be taken at multiple points during and between thermal plateaus. This shall include cold operate and hot operate regimes and periods when transitioning from cold to hot or visa versa. The spectra shall be acquired using the RAS/Cal Pt/Ne lamps and using the on-board wavelength calibration lamps.
- Each data set shall be reduced following the algorithms presented in section 4 of this document to create a final extracted spectrum.
- The locations of emission lines shall be compared between the RAS/Cal science spectra and the wavelength calibration spectra.
- The wavelength calibration spectra and RAS/Cal science spectra shall be compared between data sets acquired at different times in the thermal vacuum test profile.

The effect of the in-flight jitter cannot be characterized during ground testing, since under normal operating scenarios there is no known source of high frequency vibration within the instrument. However, during ground testing it is desirable to test for jitter to support SMOV-4 activities. Therefore, an attempt shall be made to detect jitter. Either way, this test and associated data will form a data set for comparison with the SMOV-4 activity associated with characterizing jitter in orbit (see section 6.9). Jitter shall be measured as follows:

- Using the data acquired for purposes of characterizing the drift of the spectrum, measure the FWHM of identical emission lines from the wavelength calibration lamps and the RAS/Cal Pt/Ne lamps.
- Using the data acquired during focus testing (see section 5.6) measure the FWHM of identical emission lines from the wavelength calibration lamps and the RAS/Cal Pt/Ne lamps at each focus position.
- Compare the FWHMs of the lines acquired from each lamp and for each focus position.

If jitter is present somewhere in the system the FWHMs of the lines will be dissimilar, however, it is impossible to predict which lamp will show the effects of jitter. In the best

case the resolutions will be similar and shall form a data set for comparison with the in-flight measurement of jitter.

5.13 NUV IMAGING CAPABILITY

Per the "Hubble Space Telescope Cosmic Origins Spectrograph Contract End Item (CEI) Specification" (STE-63) section 4.3.9 the NUV channel TA-1 mode shall be able to distinguish two point sources of equivalent intensity that are separated by 1 arc-second. Furthermore, is shall be possible to locate a target within the aperture to better than 0.1 arc-seconds.

The ability to distinguish between two sources separated by 1 arc-second shall be demonstrated by measuring the point spread function of a point source as generated by RAS/Cal. No processing of the data shall be required prior to analyzing the data.

The requirement of being able to locate a target within the aperture to better than 0.1 arc-seconds requires observation of the point source and an observation of the wavelength calibration lamp through the TA-1 channel and in dispersed light.

- Using RAS/Cal and a monochromatic light source to generate an input point source to the COS instrument.
- Configure COS into the TA-1 mode.
- Scan the point source across the aperture in the dispersion and cross dispersion direction in increments of 0.2". In each case the scan is done through the middle of the aperture.
- At each scan point acquire an image of the target and an image of the wavelength calibration aperture using the on-board wavelength calibration lamp.
- Correlate the known position of the target at the aperture with the observed location in the NUV image and the corresponding NUV image of the wavelength calibration aperture.
- Place the image at the center of the field of view and then adjust the OSM1 and OSM2 mechanisms ±2 steps. Acquire images at each combination of OSM1 and OSM2 positions. This will require a total of 25 separate measurements.
- Place the image at the center of the field of view and position all the mechanisms in their nominal orientations.
- Introduce monochromatic light using RAS/Cal into the COS/NUV channel and measure the incident and detected photons. Repeat the efficiency measurement using different wavelengths. Wavelengths shall be chosen to sample roughly every 200-300Å.
- Reconfigure OSM2 into the "rear view mirror" mode (see OP-01 for details) and repeat the efficiency calibration.

6. IN ORBIT CALIBRATION OF COS

6.1 INTRODUCTION

This section pertains to the calibration of the entire COS instrument during SMOV-4. All reference files required to correctly reduce flight data shall be verified and updated as required.

6.2 WAVELENGTH SCALE

Each channel and associated configuration shall have a unique wavelength scale of the form shown in equation 6.2-1. The wavelength scale shall refer to the wavelength calibration spectra. A table of offsets for each channel shall be created that corrects for offsets between the wavelength calibration spectra and the science spectra. These offsets are constant and are due to differences in the illumination angle between the wavelength calibration optical path and the science optical path and the physical location of the wavelength calibration aperture with respect to the primary science aperture.

$$\lambda(P_x) = a_0 + a_1 P_x + a_2 P_x^2 + a_3 P_x^3 + \Delta a_{channel} \qquad \text{Eqn. 6.2-1}$$

where

P_x is the Doppler corrected pixel value in the dispersion axis
$a_{0\text{-}3}$ are coefficients contained in the appropriate reference file
λ is the wavelength in Å
$\Delta a_{channel}$ is the offset required to calculate the science spectrum wavelength scale. $\Delta a_{channel} = 0$ for all wavelength calibration spectra and is non zero for science spectra.

The wavelength scale for each channel and configuration shall be determined as follows:

- Acquire a wavelength calibration spectrum in TTAG mode with a minimum of 1000 counts in at least 20 emission lines using the onboard wavelength calibration lamps.
- If the spectrum is an FUV spectrum then correct the detector image for thermal distortion (section 4.3) and geometric distortions (section 4.4).
- Create a 2-D image following the algorithm shown in section 4.12.1.
- Extract the image following the section 4.13.1 for the FUV or section 4.13.2 for the NUV channels.

- Fit gaussian line profiles to as many lines as possible and record the centroid for each gaussian profile. Each emission line shall have a minimum of 1000 counts total in the emission line.
- Using the Pt/Ne line list published in ApJ (Reader *et al* 1990, ApJ, **72**, 831) identify the emission lines.
- Use a least squares routine fit a polynomial of the form shown in 5.3-1 to the centroid versus wavelength data.

The constant offsets between the wavelength calibration scale and the science wavelength calibration shall be determined as follows:

- Acquire a wavelength calibration spectrum in TTAG mode with a minimum of 1000 counts in at least 20 emission lines using the onboard wavelength calibration lamps.
- Acquire a spectrum of a standard star with known interstellar absorption lines. The object shall be centered in the primary science aperture to within 30 μm (0.1" in the HST focal plane).
- If the spectrum is an FUV spectrum then correct the detector image for thermal distortion (section 4.3) and geometric distortions (section 4.4).
- Create a 2-D image following the algorithm shown in section 4.12.1.
- Extract the image following the section 4.13.1 for the FUV or section 4.13.2 for the NUV channels.
- Apply the wavelength scale appropriate for that channel and configuration to both data sets.
- Fit gaussian line profiles to as many lines in each spectrum as possible and record the central wavelengths.
- Compare the observed wavelengths for the absorption lines against the known wavelengths. The difference in the wavelengths shall be the $\Delta a_{channel}$.
- Record this number for the channel being evaluated.

It is highly unlikely that there will be a significant difference between the $\Delta a_{channel}$ derived during ground calibration and during SMOV-4.

6.3 FOCUS CALIBRATION

Each optic on the OSM1 shall undergo a focus test. For the FUV channel a single central wavelength position for each grating is adequate. For the NUV channels the G185M and TA1 channels shall be used. The purpose of this calibration is to record the focus performance of the instrument versus position of the linear translation mechanism on OSM1. At each discrete position of the linear translation mechanism a wavelength calibration spectrum shall also be acquired.

The focus calibration shall be conducted as follows:

- Acquire a wavelength calibration spectrum in TTAG mode with a minimum of 1000 counts in at least 20 emission lines using the onboard wavelength calibration lamps.
- Acquire a spectrum of a standard star with interstellar absorption lines. The object shall be centered in the primary science aperture to within 30 μm (0.1" in the HST focal plane).
- If the spectrum is an FUV spectrum then correct the detector image for thermal distortion (section 4.3) and geometric distortions (section 4.4).
- Create a 2-D image following the algorithm shown in section 4.12.1.
- Extract the spectra following the section 4.13.1 for the FUV or section 4.13.2 for the NUV channels.
- Apply the wavelength scale appropriate for that channel and configuration to both data sets.
- Fit gaussian line profiles to as many lines in each spectrum as possible and record the central wavelengths.
- Reposition the linear stage and repeat until the full travel of the linear translation mechanism has been covered. The linear translation mechanism position shall be incremented in 0.5 mm steps, for a total of 28 science and 28 wavelength calibration exposures.

Each exposure shall be analyzed as follows:

- For each position of the linear translation mechanism, plot the 1 σ width for each line versus the centroid pixel.
- Compare the 1 σ width versus centroid pixel for each position of the linear translation mechanism. The plot with the lowest average 1 σ shall identify the optimum position of the linear translation mechanism.

6.4 SPECTRAL RESOLUTION

The spectral resolution of each channel and configuration shall be measured after the best focus is identified for each channel. The spectral resolution shall be measured using the widths of unsaturated interstellar absorption lines. The interstellar absorption lines shall be unsaturated and relatively weak. Furthermore, it is advantageous to use absorption lines with simple velocity structures to avoid broadening due to unresolved complexes or blends. In addition, the spectral resolution of wavelength calibration spectra for each configuration shall also be measured. Spectral resolution is defined per the "Hubble Space Telescope Cosmic Origins Spectrograph Contract End Item (CEI) Specification"

(STE-63) in section 4.3.2 "as the ratio $R=\lambda/\Delta\lambda$, where λ is the wavelength, and $\Delta\lambda$ is the measured Full Width at Half Maximum of a spectral feature whose intrinsic width is much narrower than the instrumental broadening." The spectral resolution for a single channel and configuration shall proceed as follows:

- Acquire a spectrum with 1000 counts per resolution element of a standard star with known unsaturated interstellar absorption lines. The object shall be centered in the primary science aperture to within 30 μm (0.1" in the HST focal plane).
- Acquire a spectrum of the wavelength calibration lamp in TTAG mode. For the FUV channels there shall be a minimum of 1000 counts in at least 20 emission lines using the onboard wavelength calibration lamps. For the NUV channels there shall be a minimum of 3 lines per spectral stripe and 9 total with at least 1000 counts in each line.
- If the spectrum is an FUV spectrum then correct the detector image for thermal distortion (section 4.3) and geometric distortions (section 4.4).
- Create a 2-D image following the algorithm shown in section 4.12.1.
- Extract the image following the section 4.13.1 for the FUV or section 4.13.2 for the NUV channels.
- Fit gaussian line profiles to as many lines as possible and record the 1 σ width and centroid for each emission line. Each emission line shall have a minimum of 1000 counts total in the emission line.
- Form the ratio $R= \lambda/\Delta\lambda$ for the wavelength calibration spectrum and the absorption line science spectrum.
- Compare the resolution versus wavelength between the preflight and in-flight wavelength calibration spectra.
- Compare the resolution of the absorption lines in the spectrum of the science target.

6.5 SPATIAL RESOLUTION

Per the "Hubble Space Telescope Cosmic Origins Spectrograph Contract End Item (CEI) Specification" (STE-63) section 4.3.3, "COS shall be capable of producing separate and distinguishable spectra for two point sources whose separation in the aperture is greater than 1.0 arc seconds." This specification applies to each channel as well. The spatial resolution of COS shall be verified at a minimum by characterizing the astigmatic height of the spectrum as a function of wavelength for each channel for a point source with a continuum spectrum. By analysis it shall be shown that two objects separated by more than 1 arc-second shall produce separate and distinguishable spectra. If possible, multiple astronomical targets with separations less than and greater than 1 arc-second shall be observed to verify the spatial resolution of the COS channels. In this case the

science targets shall be oriented such that the line between the targets is perpendicular to the dispersion plane of the instrument.

6.6 SENSITIVITY CALIBRATION

Each channel and associated configuration shall be calibrated for efficiency for a total of 16 FUV configurations and 54 NUV configurations per OP-01 (see Tables 2.1-1 and 2.1-2). The efficiency shall be expressed in units of (counts/sec)/(ergs/sec/Å/cm^2). The efficiency for a given channel and configuration shall be measured as follows:

- Observe in TTAG mode any one of a variety of standard stars. The observation shall consist of 4 FP Split exposures each with a signal to noise ratio of 30:1.
- Correct the data back to the Baseline Reference Frame following the algorithm described in section 4.3.
- Correct the data for geometric distortions following the algorithm described in section 4.4.
- Calculate and assign the ε correction factors to each photon per section 4.7.
- Correct the data for Doppler induced shifts per section 4.9.
- Resample the image into a 2-D array following the algorithm described in section 4.12.1.
- Extract the spectrum following the section 4.13.1 for the FUV or section 4.13.2 for the NUV channels.
- Divide the observed spectrum in units of effective counts per second by the spectrum of the standard star in units of ergs/sec/Å/cm^2 that has been sampled identically to the flight spectrum. The resultant quantity is the efficiency curve for that channel and configuration.

The wavelength dependent efficiency of the BOA aperture shall be calibrated. The efficiency of the BOA shall be measured by observing a star with a predominantly continuum spectrum in the PSA. The same star shall then be observed using the BOA. The efficiency calibration shall be the BOA spectrum divided by the PSA spectrum.

Both modes of the TA-1 channel sensitivity shall be calibrated by observing a series of standard stars of various spectral classifications. These stars shall also be observed with the bright object aperture.

6.7 FLAT FIELD RESPONSE

The flat field response shall be determined using the onboard flat field lamp and using a standard star with a predominantly continuum spectrum. This will allow the IDT to better understand the flat field performance derived from the onboard calibration lamps and from a stellar source. The results shall then be compared for consistency and any

differences shall be studied and recorded to support the potential need for using stellar sources to derive flat fields in the event that the onboard flat field calibration lamps fail.

The requirements for the flat field data are derived from a variety of documents that address the basic operational requirements of COS down to the practical implications of making flat field observations. Specifically, these are GSFC "Hubble Space Telescope Cosmic Origins Spectrograph Contract End Item (CEI) Specification" (STE-63), CU/CASA Technical Evaluation Report "FUV Detector Lifetime Estimates for Observation Planning" (COS-11-0018), and BASD Systems Engineering Reports "COS Signal to Noise Ratio and Flat Field Issues" (COS-Cal-001) and "Strategies for High Signal to Noise Ratio COS Spectra" (COS-Cal-008).

The primary requirement placed on the flat field data is that the signal to noise of the data shall be greater than or equal to 70:1 at the resolution element level. This assumes an observation that requires a signal to noise of 100 shall be comprised of four sub-exposures each with a signal to noise of 70:1 (COS-Cal-008). The large number of pixels provided by the detector makes it impractical and potentially detrimental to measure the flat field response at the pixel level due to concerns over the total exposure time (on order 50 hours) and the total charge extracted from the microchannel plate detectors (COS-11-0018).

The deuterium lamps onboard COS cover from 1150Å to 3200Å. At the shortest wavelength the deuterium lamp emits a dense forest of lines, which when blurred by the flat field aperture, forms a pseudo continuum. A 2Å resolution spectrum of a deuterium lamp is shown in figure 5.8-1 and is representative of what we can expect using the onboard flat field calibration system. This figure demonstrates that the flat field maps for each segment of the FUV detector will have to be created using different modes. Specifically, the flat field for segment A of the FUV detector shall be created using the G140L grating and that the flat field map for segment B shall be created using the G160M grating. The flat fields maps for the NUV grating shall be done using the G185M grating where the fluxes are fairly uniform with no strong features in the continuum spectrum. Figure 5.8-2 shows the spectral distributions across each segment of the FUV detector.

Independent of the method used to introduce the light, either onboard system or a stellar source, the resolution element to resolution element response of the instrument shall be created as follows:

- Acquire a time tag data set with a minimum of 80 events per pixel or a minimum total number of events in the spectral region of 52,062,500. This will require about 2.5 hours of observation at 20,000 events/second.

- Correct the data back to the Baseline Reference Frame following the algorithm described in section 4.3.
- Correct the data for geometric distortions following the algorithm described in section 4.4.
- Resample the image into a 2-D array following the algorithm described in section 4.12.1.
- Create an L-fit by fitting a 2-D polynomial function of at least 10 degrees of freedom to the data. The L-fit shall replicate the low-frequency behavior of the spectrum to TBD%.
- Divide the L-fit into the raw 2-D image to create a P-flat. The P-flat will then contain values on order unity.
- Smooth the P-flat data in both the dispersion and cross-dispersion directions using

On-orbit flat fields derived using stellar sources shall be acquired using the same configurations as those used with the on-board calibration lamps. However, during SMOV-4 flat field data shall also be acquired using each channel in at least one configuration. These data shall be used to confirm that it is appropriate to apply flat field data derived from G140L, G160M, and G185M data to other spectroscopic channels.

6.8 SIGNAL TO NOISE

Per the "Hubble Space Telescope Cosmic Origins Spectrograph Contract End Item (CEI) Specification" (STE-63) section 4.3.5, during instrument level calibration it shall be demonstrated that a signal to noise of 100:1 is possible. The signal to noise ratio of 100:1 shall be demonstrated at a minimum by using 4 sub-exposures that are then processed and co-added. Each sub-exposure shall be taken with the OSM1 mechanism is a slightly different configuration. At a minimum a signal to noise of 100:1 shall be demonstrated in a high resolution FUV mode and a high resolution NUV mode. The demonstration shall follows the steps below.

- Acquire in TTAG mode 4 70:1 signal to noise spectra of any one of a variety of standard stars, which have highly saturated absorption lines.
- Correct the data back to the Baseline Reference Frame following the algorithm described in section 4.3.
- Correct the data for geometric distortions following the algorithm described in section 4.4.
- Calculate and assign the ε correction factors to each photon per section 4.7.
- Correct the data for Doppler induced shifts per section 4.9.
- Resample the image into a 2-D array following the algorithm described in section 4.12.1.

- Extract the spectrum following the section 4.13.1 for the FUV or section 4.13.2 for the NUV channels.
- Co-add the spectra.
- Calculate the reciprocal of the root-mean-square (RMS) scatter of data points about a smooth function fit to those points away from the absorption line (N).
- The signal shall be calculated by subtracting off the flux as measured at the bottom of the absorption line from the continuum level (S).
- The signal to noise ratio is then the ratio of S/N.
- Other strategies may also be used for comparison purposes.

6.9 CALIBRATION LAMP INTENSITY

There are four calibration lamps onboard the COS calibration delivery system, 2 Pt/Ne wavelength calibration lamps and 2 deuterium flat field lamps. The optical paths for each lamp are unique with slightly different efficiencies. In addition, each lamp can be operated at 3 current levels. Therefore, there are a total of 6 different intensity levels available for wavelength calibration and flat field calibration. Each of these intensity levels shall be calibrated for future reference to monitor the degradation of the calibration subsystem performance due to contamination.

In addition, the intensity of the lamp versus time shall be measured for the minimum current level over a 10-minute period.

The configurations that shall be calibrated are presented in table 6.9-1.

Table 6.9-1

Lamp	Current Levels
Pt/Ne #1	**low**, medium, *high*
Pt/Ne #2	**low**, medium, *high*
D2 #1	**low**, medium, *high*
D2 #2	**low**, medium, *high*

bold text indicates the preferred current levels
italic text indicates current levels to avoid under normal circumstances or where the potential for permanently damaging the instrument exists.

The calibrations shall proceed as follows:

- Configure COS into the G160M mode.
- With the COS instrument on and ready to acquire data turn on a calibration lamp at the minimum current level and acquire a TTAG data set for 10 minutes.
- Then increase the lamp current to the intermediate setting and acquire a TTAG data set for 5 minutes.
- Finally, increase the current level to the maximum setting and acquire a TTAG data set for 5 minutes.
- Repeat this process for each lamp.
- Reconfigure COS into the G185M mode and repeat the above steps.

6.10 STRAY & SCATTERED LIGHT

Scattered light is defined as polychromatic light incident on the detector active area that originates from the diffractive surface of the grating in the optical path. Per the "Hubble Space Telescope Cosmic Origins Spectrograph Contract End Item (CEI) Specification" (STE-63) section 4.3.7 the stray and scattered light shall constitute less than "2% residual intensity to the signal in the core of a saturated absorption line measured with any of the high dispersion modes (GnnnM) in the spectrum of a point source in the PSA". The scattered light shall be measured by observing saturated absorption lines in the spectrum of a hot star, e.g. an O or B star.

The stray and scattered light shall be measured as follows:

- Observe in TTAG mode a standard star with known highly saturated interstellar absorption lines that have flat bottoms over several resolution elements..
- Correct the data back to the Baseline Reference Frame following the algorithm described in section 4.3.

- Correct the data for geometric distortions following the algorithm described in section 4.4.
- Calculate and assign the ε correction factors to each photon per section 4.7.
- Correct the data for Doppler induced shifts per section 4.9.
- Resample the image into a 2-D array following the algorithm described in section 4.12.1.
- Extract the spectrum following the section 4.13.1 for the FUV or section 4.13.2 for the NUV channels.
- Compare the continuum level to the level of the signal at the bottom of the absorption line.
- Using the fully corrected image examine the image for stray light.
- Repeat measurement for each grating.

6.11 STABILITY & REPEATABILITY

Per the "Hubble Space Telescope Cosmic Origins Spectrograph Contract End Item (CEI) Specification" (STE-63) section 4.3.8 changes in the position of the spectrum that occur on long time scales (>1 hr), referred to as drift, shall be less than 1 resolution element per hour. Furthermore, knowledge of the drift shall be provided that allows drift to be corrected to < 0.25 resolution elements. Changes in the position of the spectrum on short time scales (<1 hr), referred to as jitter, shall not "contribute more than 0.25 resolution elements to the FWHM" of a resolution element.

Drift is due to changes in the position of any component in the optical path, thermal distortions in encoding the position of a photon, and many other unspecified effects. Jitter is due to random variations on short time scales and is dominated by high frequency pointing errors and vibration effects associated with the HST spacecraft.

During SMOV-4 drift shall be characterized as follows:

- The HST shall acquire and track a known calibration star with narrow emission or absorption lines. The calibration star absorption or emission features shall have no time variable component, e.g. Doppler shifts.
- Wavelength calibration spectra shall be acquired at 10-minute intervals during the 10 orbits of science observation.
- Each data set shall be reduced following the algorithms presented in section 4 of this document to create a series of spectra.
- The locations of Pt/Ne emission lines shall be determined by fitting gaussian profiles to at least 20 lines across the observed wavelength region.
- The locations of the known emission or absorption lines shall be determined by fitting gaussian profiles to the available lines.

- The wavelength calibration spectra shall be compared for consistency between the locations of the observed emission lines in the Pt/Ne spectra.
- The centroid positions of the emission lines of the wavelength calibration spectra shall be compared to the observed centroids of the emission or absorption lines in the calibration star spectra.
- Any time dependent deviation shall be called drift.

Jitter cannot be directly measured and must be inferred from an evaluation of the resolution of the instrument and will affect the resolution of the instrument in a similar fashion for all spectroscopic channels. There are no unique observations that can isolate the effects of jitter other than a comparison of the pre- and in-flight FWHMs between the wavelength calibration spectra and the observed FWHMs of narrow emission or absorption lines in the spectrum of a point source object. The data required for this analysis is acquired during focus testing, so no unique observations are required to evaluate the effects of jitter.

6.12 NUV IMAGING CAPABILITY

Per the "Hubble Space Telescope Cosmic Origins Spectrograph Contract End Item (CEI) Specification" (STE-63) section 4.3.9 the NUV channel TA-1 mode shall be able to distinguish two point sources of equivalent intensity that are separated by 1 arc-second. Furthermore, is shall be possible to locate a target within the aperture to better than 0.1 arc-seconds.

The ability to distinguish between two sources separated by 1 arc-second shall be demonstrated by measuring the point spread function of an astronomical point source. No processing of the data is required prior to analyzing the data.

The requirement of being able to locate a target within the aperture to better than 0.1 arc-seconds requires observation of the point source and an observation of the wavelength calibration lamp through the TA-1 channel and in dispersed light. The 0.1 arc-second requirement is necessary to meet the absolute wavelength scale accuracy requirement of 15 km/sec.

- Configure COS into the TA-1 mode.
- Acquire an astronomical target with a known spectrum.
- Acquire an image of the astronomical target.
- Acquire an image of the wavelength calibration aperture using the on-board wavelength calibration lamp.
- Reconfigure COS into an appropriate NUV spectroscopic mode (GXXXM) and acquire a spectrum of the target.

- Using the standard data reduction algorithms extract the spectrum of the target.
- Compare the measured wavelengths with the known wavelengths.
- Compare the TA-1 image with the measured preflight relationship between the target's position in the aperture with the location of the wavelength calibration aperture.

6.13 APERTURE RELATIONSHIPS

After installation of COS into the HST the relationship between the location of the PSA and the HST coordinate system shall be calibrated. The calibration shall be conducted as follows:

- Configure the COS instrument into the TA-1 image mode.
- Acquire an astronomical target. Because the relationship between the PSA and the HST coordinate system has not yet been calibrated this step may require raster type scan to place the target within the center of the PSA.
- After the target has been placed within the PSA aperture, begin scanning the target across the entire aperture along the V2 axis of the HST coordinate system. Each dwell point shall be separated by 0.25 arc-seconds and shall cover a total of 6 arc-seconds. At each dwell point acquire a TA-1 image.
- Place the target at the center of the aperture as defined by the V2 scan and repeat the scan along the V1 axis.
- Place the target at the center of the aperture as defined by the V1 scan.
- Repeat the scans along the V1 and V2 axes.

These data shall be used to calibrate:

- The magnitude of the observed motion of the image versus the programmed motion.
- The direction of observed motion versus programmed motion.
- The count rate versus position within the PSA.
- The optimum position of a target in the HST coordinate system (V1, V2).

6.14 TARGET ACQUISITION

After the aperture relationship is calibrated, see section 6.13, it shall be necessary to exercise all the target acquisition algorithms and verify all the target acquisition parameters, e.g. sub-arrays for the spectrum, geocoronal emission lines, and wavelength calibration aperture. The accuracy of the target acquisition based on spectral content shall be measured against the target acquisition algorithms based on the TA-1 image mode.

6.15 DOPPLER AMPLITUDE

The maximum amount of Doppler motion for each channel is an input to the flight software that controls the Doppler compensation in ACCUM mode. The maximum Doppler motion shall be verified by observing an astronomical point source with intrinsic emission lines that lies near or on a tangent of the HST orbital plane. In TTAG mode acquire a spectrum of the target for at least 1 full orbit. The target shall have sufficient flux to support breaking the data set into at least 6 subsets for time-based analysis (assuming 30 minute visibility, each subset will have a 5 minute exposure time). For each time segment measure the centroid of at least one emission line and then plot the centroid versus time. Fit a sinusoidal function to the data and determine the maximum amplitude.

6.16 DETECTOR PROPERTIES

The detector dark rate shall be measured as a function of geomagnetic coordinates. This shall be done by acquiring data in TTAG mode and relating the global count rate with respect to the Earth's magnetic field. In addition, over time the SAA contour used to plan the ramping of the COS detectors high voltage shall be slowly decreased until such a point as the SAA is actually detected. The SAA contour shall then be increased such that sufficient margin exists to support normal HST operations.

7. DERIVATIONS & PROOFS

7.1 DERIVATION OF EQUATION 4.13-6

The detector background, not sky background, for the FUV and NUV detectors is formed through a combination of several sources. These sources include radioactive decay of material within the microchannel plate, cosmic rays, charged particle, and photons, which originate from a variety of sources including fluorescence of the MgF_2 window and stray light. In the absence of external influences, such as a vignetting element, it is largely impossible to distinguish the source of a detected event. Even if an event can be identified as a background event, the source of that background event cannot be identified. Therefore, the question is how can the contribution to the detected signal from background be estimated and corrected.

The detected events for a single resolution element can be expressed as the sum of the various components that contribute to the detected signal (Equation 1).

$$D = \frac{S_\nu}{\varepsilon} + \frac{B_\nu}{\varepsilon} + \frac{B_\gamma}{\varepsilon_\gamma} + \frac{B_{cr}}{\varepsilon_{cr}} + \frac{B_{cp}}{\varepsilon_{cp}} \qquad \text{Eqn. 7.1-1}$$

where

D is the detected events
S_ν is the incident photons onto the detector from the grating.
B_ν is the incident photons onto the detector from sources other than the grating (e.g. stray light, fluorescence, etc.).
B_γ is the events due to radioactive decay in the microchannel plates themselves
B_{cr} is the events due to cosmic rays.
B_{cp} is the events due to other charged particles.
ε is the inefficiency factor derived in section 4.6 that includes flat field effects and live time corrections and will generally be ≥ 1.
ε_γ, ε_{cr}, & ε_{cp} are the inefficiency factors for radioactive decay, cosmic rays, and charged particles.

The final flux value is based on the value of S_ν, the number of photons incident onto the detector. Rearranging equation 1 to solve for S_ν we get equation 2.

$$S_\nu = \varepsilon\left(D - \left\lceil \frac{B_\nu}{\varepsilon} + \frac{B_\gamma}{\varepsilon_\gamma} + \frac{B_{cr}}{\varepsilon_{cr}} + \frac{B_{cp}}{\varepsilon_{cp}} \right\rceil\right) \qquad \text{Eqn. 7.1-2}$$

Equations 7.2-1 and 7.2-2 make an assumption worth mentioning for completeness, all sources of background are uniformly distributed across the relevant scale and that ε_γ, ε_{cr}, & ε_{cp} are constant across the relevant regions of interest., e.g. a pixel or resolution element. The expression for the incident photons, S_ν, simplifies into two different forms under two conditions. If the background is dominated by spurious photons, as would be the case for the STIS band 1 MAMA detector, then the expression reduces to equation 3. In this case, measuring the counts in an unused region of the detector and correcting for flat field and detector live time to those events determines B_ν.

$$S_\nu = \varepsilon D - B_D = \varepsilon D - \varepsilon' B'_D \qquad \text{Eqn. 7.1-3}$$

where

D, S_ν, & ε are the same as those in equation 1
B_D is the detected background events within a spectral region
ε' & B'_D refer to the inefficiency factor and detected counts for a region outside the spectral region or region of interest.

However, this assumption is not correct for COS, because, as mentioned above, we cannot distinguish between the sources of different events nor can we anticipate now that the background will be dominated by a particular source. Furthermore, the flat field lamps will not illuminate the detector outside of the spectral region, so even if the

background were dominated by stray light it would be impossible to compute B_ν. Therefore, we must treat all sources of background equally. In doing so we can combine all the sources of background into a single term, B_D, the total background (see Equation 4).

$$B_D = \frac{B_\nu}{\varepsilon} + \frac{B_\gamma}{\varepsilon_\gamma} + \frac{B_{cr}}{\varepsilon_{cr}} + \frac{B_{cp}}{\varepsilon_{cp}} \qquad \text{Eqn. 7.1-4}$$

As mentioned before, in the absence of externally imposed conditions, it is impossible to identify the source of an event, source photon or background event. However, in the case of a spectrograph, the spectrum is confined to fall within a specific region. Events that fall outside that region are identified as background events and can be used to estimate the background within the spectral region. For COS the detector background events within the spectral region will be estimated by averaging the number of events per unit area that occur directly above and below the spectral region and scaling by the ratio of the relevant areas.

Substituting B into Equation 7.2-2 we find the final functional form for correctly computing the number of events to the spectrum (Equation 7.2-5).

$$S_\nu = \varepsilon(D - B_D) \qquad \text{Eqn. 7.1-5}$$

7.2 DERIVATION OF EQUATION 4.13-7

The error term of n_i is derived as follows starting with the first expression for n_i in equation 7.2-1. Please note that these errors are derived in counts, not count rate. Lower case letters refer to counts while upper case letters refer to count rates.

$$\sigma_{n_i}^2 = \left(\frac{\delta n_i}{\delta \varepsilon_i}\sigma_{\varepsilon i}\right)^2 + \left(\frac{\delta n_i}{\delta gc_i}\sigma_{gc_i}\right)^2 + \left(\frac{\delta n_i}{\delta bk_i}\sigma_{bk_i}\right)^2 \qquad \text{Eqn. 7.2-1}$$

where

n_i is the net counts detected in spectral bin i.
gc_i is the gross counts detected in spectral bin i.
bk_i is the background counts computed for spectral bin i.
$\sigma_{\square\square}$ is the error in the counts in spectral bin i.

$$\sigma_{n_i}^2 = \left((gc_i - bk_i)\sigma_{\varepsilon i}\right)^2 + \left(\varepsilon_i \sigma_{gc_i}\right)^2 + \left(\varepsilon_i \sigma_{bk_i}\right)^2 \qquad \text{Eqn. 7.2-2}$$

Substituting equation 4.13-6 into equation 7.2-2 and combining terms results in equation 7.2-3.

$$\sigma_{n_i}^2 = \left(n_i \frac{\sigma_{\varepsilon_i}}{\varepsilon_i} \right)^2 + \varepsilon_i^2 \left(\sigma^2{}_{gc_i} + \sigma^2{}_{bk_i} \right) \qquad \text{Eqn. 7.2-3}$$

The expressions for σ_{gci} and σ_{bki} are based on Poisson noise.

$$\sigma_{g_i} = \sqrt{gc_i} \qquad \text{Eqn. 7.2-4}$$

$$\sigma_{b_i} = \sqrt{\frac{\Delta n}{\Delta w \Delta n_2} bk_i} \qquad \text{Eqn. 7.2-5}$$

Substituting equations 7.2-4 and 7.2-5 into equation 7.2-3 results in equation 7.2-6.

$$\sigma_{n_i}^2 = \left(n_i \frac{\sigma_{\varepsilon_i}}{\varepsilon_i} \right)^2 + \varepsilon_i^2 \left(gc_i + \frac{\Delta n}{\Delta w \Delta n_2} bk_i \right) \qquad \text{Eqn. 7.2-6}$$

The final issue is to determine the error associated with the ε_i term. ε□ is the weighted average of all the ε terms that fell within the spectral bin i as shown in equation 4.13-5. Equation 4.7-1 shows that ε is inversely proportional to the flat field response (ff) and the live time correction (LT which varies between 0 and 1). If the live time component is considered to be error free, which is reasonable, then the flat field is the only term that needs to be considered.

$$\varepsilon_{ij} = \frac{1}{ff_{ij} \cdot LT} \qquad \text{Eqn. 7.2-7}$$

$$\sigma_{\varepsilon_{ij}} = \frac{1}{ff_{ij} \cdot LT} \frac{\sigma_{ff_{ij}}}{ff_{ij}} = \varepsilon_{ij} \frac{\sigma_{ff_{ij}}}{ff_{ij}} \qquad \text{Eqn. 7.2-8}$$

The issue is now what is the error in flat field. The flat field in pixel i,j can be expressed as shown in equation 7.2-9.

$$ff_{ij} = \frac{c_{ij}}{\langle c \rangle} \qquad \text{Eqn. 7.2-9}$$

Where c_{ij} is the number of counts in the flat field image at pixel i, j. The local average, <c>, is expressed as:

$$\langle c \rangle = \frac{1}{N} \sum_{i,j} c_{ij} \qquad \text{Eqn. 7.2-10}$$

N is the number of pixels used to form the local average. The expression for the error in the flat field, σ_{ff}, is then:

$$\sigma^2_{ffij} = \left(\frac{\sigma_{cij}}{\langle c \rangle} \right)^2 + \left(ff_{ij} \frac{\sigma_{\langle c \rangle}}{\langle c \rangle} \right)^2 \qquad \text{Eqn. 7.2-11}$$

The σ_{cij} term is simply the square root of the counts in the pixel i,j. The error in the local average, <c>, is shown in equation 7.2-12.

$$\sigma_{\langle c \rangle} = \frac{1}{N} \sqrt{\sum_{i,j} \left(\sigma^2_{cij} \right)} \approx \frac{1}{\sqrt{N}} \sigma_{cij} \qquad \text{Eqn. 7.2-12}$$

So, as the number of pixels used to form the average, N, increases the error of $\sigma_{<c>}$ decreases. Since the ff_{ij} is of order unity and N is > 60 (the number of pixels in one resolution element), the dominant term in equation 7.2-11 is the first term. Dividing equations 7.2-9 and 7.2-11 assuming that the error in the $\sigma_{<c>}$ is small we get equation 7.2-13

$$\frac{\sigma_{ffij}}{ff_{ij}} = \frac{\sigma_{cij}}{c_{ij}} \qquad \text{Eqn. 7.2-13}$$

Combining equations 7.2-8 and 7.2-13 we arrive at the following expression.

$$\frac{\sigma_{\varepsilon ij}}{\varepsilon_{ij}} = \frac{\sigma_{ffij}}{ff_{ij}} = \frac{\sigma_{cij}}{c_{ij}} = \frac{1}{SNR_{ffij}} \qquad \text{Eqn. 7.1-14}$$

We now see that $\sigma_\varepsilon/\varepsilon$ is really just the inverse of the signal-to-noise (SNR) of the counts per pixel used to compute the flat field response. This term may be used as a constant rather than a variable since it really is a statement of how well we understand the flat field response. It is also obvious that the more accurately we know the flat field response, the less important it is in the total noise, as it should be.

One last point needs to be made. In equation 7.2-6 the subscript i refers to a spectral bin or column, which is the average of all the rows, j, along the column i. Thus, the knowledge of ε_i is further improved as is shown in equation 7.2-15.

$$\frac{\sigma_{\varepsilon_i}}{\varepsilon_i} = \frac{1}{N_j}\sum_j \frac{\sigma_{\varepsilon_{ij}}}{\varepsilon_{ij}} \approx \frac{1}{N_j \cdot SNR_{ffij}} \qquad \text{Eqn. 7.2-15}$$

where

N_j is the number of rows.

Thus, the natural averaging along a column further minimizes the error associated with the knowledge of the flat field. The final form of the error for the raw spectrum in counts per second is then given by equation 7.2-16 and is equivalent to equation 4.13-16. Note that the lower case values gc, bk, and n have been replaced by GC, BK, and N all multiplied by the exposure times and that that the error in the counts has also been divided by the exposure time to put the error in the correct units of counts/second.

$$\sigma_{N_i} = \frac{1}{t_{\exp}}\sqrt{\left(N_i t_{\exp}\frac{1}{N_j \cdot SNR_{ff_{ij}}}\right)^2 + \varepsilon_i^{\,2} t_{\exp}\left(GC_i + \left(\frac{\Delta n}{\Delta w \Delta n_2}\right)BK_i\right)} \qquad \text{Eqn. 7.2-16}$$